Available online at www.sciencedirect.com
SCIENCE DIRECT®
Deep-Sea Research I 52 (2005) 2109–2139
DEEP-SEA RESEARCH PART I
www.elsevier.com/locate/dsr

^{234}Th, ^{210}Pb, ^{210}Po and stable Pb in the central equatorial Pacific: Tracers for particle cycling

James W. Murray*, Barbara Paul, John P. Dunne[1], Thomas Chapin[2]

School of Oceanography, University of Washington, Box 355351, Seattle, WA 98195-5351, USA

Received 30 August 2004; received in revised form 17 January 2005; accepted 15 June 2005
Available online 11 August 2005

Abstract

Samples were collected during the 1992 US JGOFS EqPac Survey I and II cruises from 12°N to 12°S at 140°W in the central equatorial Pacific for water column profiles of dissolved, particulate and total ^{234}Th, ^{210}Pb and ^{210}Po and total acid soluble stable Pb and sediment trap fluxes of ^{234}Th, ^{210}Pb and ^{210}Po. Survey I occurred in February/March with moderate El Nino conditions while Survey II was conducted in September/October when there was a well developed cold-tongue. ^{234}Th, ^{210}Pb and ^{210}Po are all particle reactive yet they partition differently between dissolved and particulate phases. Fractionation factors (the ratios of the distribution coefficients) show that the selectivity for suspended and sediment trap particles follows Th > Po > Pb. Scavenging residence times (τ) for ^{234}Th, ^{210}Pb and ^{210}Po ranged from 25 to 100 d, 3 to 8 years and 100 to 500 d, respectively. These particle reactive tracers have very different distributions in the water column, which reflect differences in their sources and sinks. The deficiency of ^{234}Th relative to ^{238}U was fairly uniformly distributed meridionally, though deficiencies were higher during Survey II when there was higher new production. Excess ^{210}Pb relative to ^{226}Ra was very asymmetrical with much higher excess values north of the equator. The distributions were similar for Surveys I and II. The deficiency of ^{210}Po relative to ^{210}Pb had a symmetrical distribution about the equator for both Survey I and II but the deficiencies were larger during Survey I when upwelling was smaller. Stable Pb was generally higher at the surface than at 250 m and there was no meridional trend from 12°N to 12°S. A mass balance for ^{210}Pb was used to determine the atmospheric input of ^{210}Pb. The average values for Surveys I and II were 0.12 and 0.32 dpm cm^{-2} year^{-1}, respectively. There was no general increase in atmospheric input of ^{210}Pb north of the equator but there was a strong maximum at 2–3°N during Survey I coincident with the location of the intertropical convergence zone (ITCZ), suggesting a large role for wet deposition. A mass balance for stable Pb was used to determine the atmospheric input of stable Pb. Results ranged from 110 to 140 pmol cm^{-2} year^{-1}. This flux was low in the southern hemisphere and increased steadily north of the equator. We evaluated use of ^{210}Po as a tracer for export of particulate organic matter during Survey I. Organic carbon and ^{210}Po were highly correlated in suspended matter and sediment trap samples. Average values of organic carbon fluxes determined from the deficiencies of ^{210}Po times the orgC/^{210}Po ratio agreed well with those determined from the

*Corresponding author. Fax: +1 206 685 3351.
E-mail address: jmurray@u.washington.edu (J.W. Murray).
[1]Present address: NOAA/GFDL, P.O. Box 308, Forrestal Campus B site, Princeton, NJ 08542-0308, USA.
[2]Present address: US Geological Survey, P.O. Box 25046, Mailstop 973, Denver Federal Center, Denver, CO 80225, USA.

0967-0637/$ - see front matter
doi:10.1016/j.dsr.2005.06.016

deficiencies of ^{234}Th times the organic carbon/^{234}Th ratio and ^{15}N-new production, but had a much larger variability because of the more variable advection corrections.

Keywords: Radioisotopes; Lead; Scavenging; Particle cycling; Export flux; Equatorial Pacific

1. Introduction

Particle cycling and export in the upper ocean are critical biogeochemical components of the ocean's carbon balance. Because it is difficult to study these processes directly, researchers have frequently used particle reactive, radioactive tracers. Particularly, the short-lived particle reactive U–Th series isotopes ^{234}Th ($t_{1/2} = 24.1$ d), ^{210}Pb ($t_{1/2} = 22.3$ years) and ^{210}Po ($t_{1/2} = 138$ d) are useful tracers of these processes. The different half-lives and scavenging affinities of these isotopes integrate the effects of scavenging over different time scales. Their different source functions decouple their boundary conditions. Before now, there have been few studies in which all three tracers were measured on both water column and sediment trap samples at the same time.

^{234}Th is a well-studied particle reactive tracer that has been used as a tracer for scavenging (Bhat et al., 1969; Matsumoto, 1975; Honeyman et al., 1988). The deficiency of ^{234}Th in the euphotic zone, relative to its parent ^{238}U, has been used to calculate the export flux of particles and carbon (Coale and Bruland, 1985; Murray et al., 1989, 1996; Buesseler et al., 1992, 1995; Bacon et al., 1996). The partitioning of ^{234}Th between dissolved and particulate phases has been used to determine rates of sorption/desorption and aggregation/disaggregation (e.g., Honeyman et al., 1988; Honeyman and Santschi, 1989; Clegg and Whitfield, 1990, 1991, 1993; Murnane et al., 1990, 1994a, b; Dunne et al., 1997).

The radioactive deficiency of ^{210}Pb relative to its parent ^{226}Ra was first used to estimate scavenging rates in the deep sea (Craig et al., 1973) and subsequently to quantify boundary scavenging at the edges of ocean basins (Bacon et al., 1976; Spencer et al., 1981; Nozaki et al., 1997). ^{210}Pb activities are usually greater than those of ^{226}Ra in the surface ocean (e.g. Chung and Craig, 1983; Nozaki et al., 1976) because of atmospheric deposition of ^{210}Pb resulting from decay of atmospheric ^{222}Rn transported from the continents (Turekian and Cochran, 1981).

^{210}Po is typically deficient relative to its parent ^{210}Pb because of preferential biological removal (Shannon et al., 1970; Turekian et al., 1974; Kadko, 1993). Its scavenging rate appears to vary with biomass (Nozaki et al., 1998) and primary production (Kadko, 1993).

The geochemistries of stable Pb and ^{210}Pb have been compared in the Pacific by Settle et al (1982) and in the Atlantic by Boyle et al. (1986, 1994), Shen and Boyle (1988) and Sherrell et al. (1992). Because continental sources for ^{210}Pb through the atmosphere are assumed to be temporally constant, normalization of stable lead to ^{210}Pb was used to deduce the decreasing temporal trend in anthropogenic atmospheric input of stable Pb.

Tanaka et al. (1983) measured the vertical and temporal variations in ^{234}Th, ^{210}Pb and ^{210}Po in Funka Bay, Japan, and compared their rates of biological removal. ^{234}Th and ^{210}Pb had similar residence times, τ which were about half those of Po. Shimmield et al. (1995) measured all three tracers in the Bellingshausen Sea, Antarctica. The export flux of ^{210}Po was lower than ^{234}Th, possibly due to more rapid recycling of ^{210}Po. Sarin et al. (1999) and Charette and Moran (1999) measured ^{234}Th, ^{210}Pb and ^{210}Po on the same samples in the south-equatorial Atlantic. They found similar scavenging residence times of ^{210}Po and ^{234}Th. Shorter scavenging and removal residence times were attributed to high biological activity. Harada and Tsunogai (1986) measured ^{234}Th, ^{210}Pb and ^{210}Po on deep ocean trap samples (>500 m) from the NE Pacific and concluded that settling particles adsorb tracers in the order ^{234}Th $>$ ^{210}Po $>$ ^{210}Pb. Friederich and Rutgers van der Loeff (2002) combined data for ^{234}Th, ^{210}Pb and ^{210}Po with multiple regression equations of

these tracers with POC and biogenic Si to estimate carbon and silica export in the Antarctic Circumpolar Current.

Experimental studies have shown that phytoplankton and zooplankton concentrate these tracers in the order Po ≫ Pb = Th > Ra > U (Heyraud et al., 1976; Kharkar et al, 1976; Cherry and Heyraud, 1991; Fisher et al., 1983). Po appears to be enriched in cell protoplasm by active biological uptake (Stewart and Fisher, 2003a, b), whereas Th and Pb are adsorbed directly onto all particle surfaces nonspecifically. Fisher et al., (1983) hypothesized that Th (and Pb) may be better tracers for the mass flux and Po a better tracer for the organic carbon flux.

We measured the distributions of ^{234}Th, ^{210}Pb, stable Pb and ^{210}Po during the 1992 US JGOFS EqPac process study on the Survey I and Survey II cruises from 12°N to 12°S at 140°W. Survey I was conducted during El Nino conditions with relatively warm surface temperatures. There was a well developed surface cold-tongue during Survey II (Murray et al., 1994). Our analyses were conducted on dissolved, particulate and total water column samples as well as drifting sediment trap samples. Data for ^{226}Ra from the same stations is available from Ku et al (1995). In this paper, we present the ^{210}Pb and ^{210}Po data and, with previously published ^{226}Ra and ^{234}Th data, discuss particulate/dissolved partitioning and scavenging residence times of Th, Pb and Po and spatial and temporal variability in the atmospheric input of ^{210}Pb and stable Pb. Finally, we evaluate the use of ^{210}Po as a tracer for POC export as has been done previously using ^{234}Th.

2. Samples and methods

Samples were collected from 12°N to12°S at 140°W on the R./V. Thompson during EqPac Survey I (TT007; February–March, 1992) and Survey II (TT011; August–September, 1992). Stations were occupied at 12°N, 9°N, 7°N, 5°N, 3°N, 2°N, 1°N, Equator, 1°S, 2°S, 3°S, 5°S and 12°S for 1.5–2.5-day periods. The hydrographic and nutrient data for these cruises were presented by Murray et al. (1995).

Discrete water column samples were collected from the surface to 250 m using a CTD-Rosette equipped with 30-l Go-Flo bottles. Samples for total and dissolved isotopes (~20 l) were processed on deck within 8 h after collection. Samples (~50–80 l) for dissolved/particulate partitioning were filtered through either 142 mm diameter 0.50 μm Nuclepore or 0.45 μm Millipore filters before processing. Samples for stable Pb were collected with a Moss Landing Marine Laboratory (MLML) trace metal clean rosette built for the EqPac study (Sanderson et al., 1995). The flux of particles was sampled with drifting sediment traps of the PIT design (Knauer et al., 1990). Traps were deployed at 5–7 depths from 50 to 250 m. The details of trap deployment and ^{234}Th and organic carbon sample processing were given in Murray et al. (1996). The acid digestion techniques used for suspended and sediment trap samples were given in Murray et al. (1996).

^{234}Th, ^{210}Pb and ^{210}Po in both water and particulate samples were analyzed by conventional alpha and beta counting techniques. For dissolved and total water samples the water was acidified to pH 1.5 with conc. HCl, spiked with yield tracers (^{230}Th, ^{209}Po and stable Pb) and $FeCl_3$, equilibrated for at least 6 h and neutralized to pH 9 with NH_4OH. The $Fe(OH)_3$ precipitate was removed and dissolved in 9 N HCl. The isotopes were separated with a series of anion exchange columns (AG 1 × 8, 100–200 mesh) (Anderson and Fleer, 1982; Coale and Bruland, 1985). Th was eluted with 9 N HCl, Pb with 8 N HNO_3 and Po with 0.1 N HNO_3. ^{234}Th was platted by stippling while ^{210}Po was spontaneously plated onto 1 cm^2 silver discs. All the ^{234}Th chemistry and beta counting for the dissolved and total water column samples were completed at sea. The rest of the analyses were completed ashore. The chemical separations and analyses of ^{234}Th and ^{210}Po were completed within 2 months of the end of the cruise. The second counts for ^{210}Po (for ^{210}Pb) were conducted about 1 year later. Decay corrections were done after Fleer and Bacon (1984). Sediment trap samples were corrected to the time of trap deployment. The precision of the ^{234}Th analyses was 6.2% (Murray et al., 1996) while those for ^{210}Po and ^{210}Pb were 5% (Wei and Murray, 1994).

Stable Pb was determined by a flow injection method with inductively coupled plasma mass spectrometry (ICP-MS) detection (Chapin, 1997). Sample preconcentration was performed with a micro column packed with 8-hydroxyquinoline (8-HQ) immobilized on Fractogel (EM Science) by the technique of Landing et al. (1986). The detection limit (3 sigma blank) for Pb was 3.9 pM. Accuracy was verified by analysis of standard reference materials (CASS-2 and NASS-3) and by intercalibration with MLMLs measurements made by graphite furnace atomic absorption spectrophotomery (GFAAS) (K. Coale, personal communication).

Water column (4–6 l) and sediment trap samples for particulate carbon were filtered through precombusted 25 mm Whatman GF/F filters. Particulate carbon analyses were conducted with a Leeman Labs CEC 440 CHN analyzer as described by Murray et al. (1996). Total suspended matter (TSM) values were obtained by whole bottle filtration of 30 l Niskin bottles on Nuclepore filters (Chapin, 1997). The filters were lightly rinsed with distilled water then dried. After weighing the filters were rinsed with distilled water and those solutions were analyses for Cl^- to make a correction for sea salt. The data in ($mg\,m^{-3}$) are available on the US JGOFS EqPac data system.

^{238}U ($dpm\,l^{-1}$) was calculated from the ^{238}U/salinity relationship of Chen et al. (1986):

$$^{238}U = 0.071 \times \text{salinity}. \quad (1)$$

^{226}Ra (dpm/100 l) was determined at the same stations by Ku et al. (1995). We used this data and the EqPac Si data from the same samples (Murray et al., 1995) to determine the linear ^{226}Ra–Si relationship in the upper 300 m:

$$[^{226}Ra] = 0.082[Si] + 8.238 \quad (r^2 = 0.741). \quad (2)$$

Similar relationships were determined previously by Nozaki et al. (1998) in the Pacific using the GEOSECS data of Chung and Craig (1980) and by Ku and Lin (1976) in the Antarctic Ocean. We used this equation and the Si data from the bottle casts to calculate ^{226}Ra.

3. Results

The water column and sediment trap data for ^{210}Pb and ^{210}Po are given in Appendices A and B, respectively, and are available on the US JGOFS EqPac data management web site (www1.whoi.edu/jgofs.html). The water column and sediment trap ^{234}Th data were published by Murray et al. (1996). The results for POC were given by Murray et al. (1996). Several sets of duplicate and triplicate analyses were made on different trap cylinders at the same depth and the precision of these replicates for carbon, ^{234}Th, ^{210}Pb and ^{210}Po all averaged 12%. The 0.1% light level during EqPac was at a depth of 120 m and this was defined as the depth of the euphotic zone (Murray et al., 1994).

The vertical profiles of the parent–daughter relationships of total nuclide activities for all stations during Survey I are shown in Fig. 1. Those for Survey II are similar in trend and thus are not shown here. $^{234}Th/^{238}U$ ratios (Fig. 1a) in the upper 120 m (the 0.1% light level) average ~0.8. There is 50% excess in ^{210}Pb relative to ^{226}Ra above about 150 m (Fig. 1b). ^{210}Po is about 40% deficient relative to ^{210}Pb in approximately the upper 100 m (Fig. 1c).

Spatial and temporal differences in the parent–daughter relationships of these tracers are more easily seen in the meridional sections. The deficiency of total ^{234}Th ($dpm\,l^{-1}$) relative to ^{238}U ($^{234}Th_{def} = {}^{238}U - {}^{234}Th$) is shown in Fig. 2. During Survey I $^{234}Th_{def}$ was uniform at about $0.4\,dpm\,l^{-1}$, but during Survey II the deficiency was much larger, reaching $0.8\,dpm\,l^{-1}$. The deficiency was centered about the equator but had its maximum at about 3–5°S. The total integrated deficiencies ($dpm\,cm^{-2}$) are plotted in Fig. 3a to illustrate the relative homogeneous distribution during Survey I versus the minimum at the equator during Survey II with maximum deficiencies at 3°N and 5°S.

Excess total ^{210}Pb ($dpm\,l^{-1} \times 100$) (defined as $^{210}Pb_{xs} = {}^{210}Pb - {}^{226}Ra$) had a very asymmetrical distribution about the equator with much higher values to the north than to the south (Fig. 4). The excess values of $^{210}Pb_{xs}$ were mostly confined to the upper 200 m. The surface values are consistent with the surface map of the Pacific by Nozaki et al.

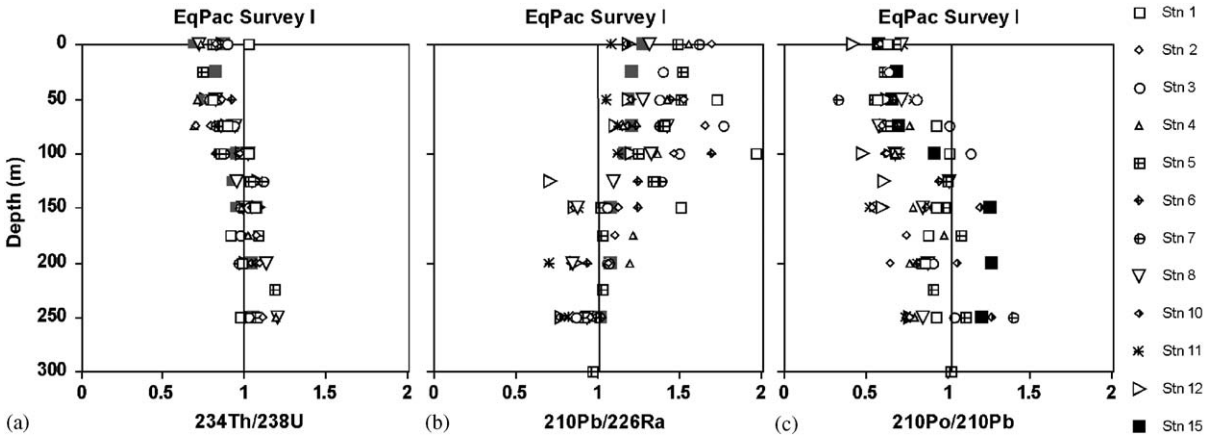

Fig. 1. Vertical profiles of the total activity ratios for (a) $^{234}Th/^{238}U$, (b) $^{210}Pb/^{226}Ra$, (c) $^{210}Po/^{210}Pb$ for Survey I for 0–250 m from 12°N to 12°S at 140°W. The vertical lines are drawn at a ratio of 1, which represents secular equilibrium.

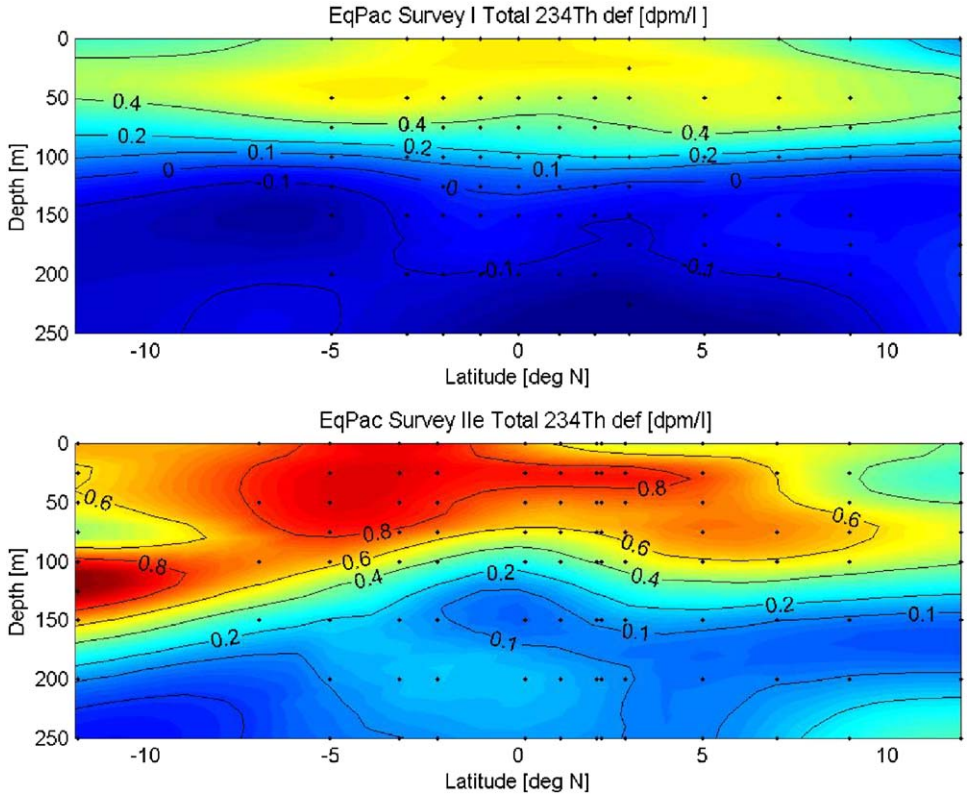

Fig. 2. Meridional section of the ^{234}Th deficiency (dpm l^{-1}) for 0–250 m from 12°N to 12°S at 140°W: (a) Survey I; (b) Survey II.

(1976). Integrated values of $^{210}Pb_{xs}$ (dpm cm^{-2}) also showed increasingly higher values north of the equator (Fig. 3b) reflecting the larger source of $^{210}Pb_{xs}$ in the northern hemisphere. The values for Survey I (which occurred during El Nino conditions) were generally higher than for Survey II,

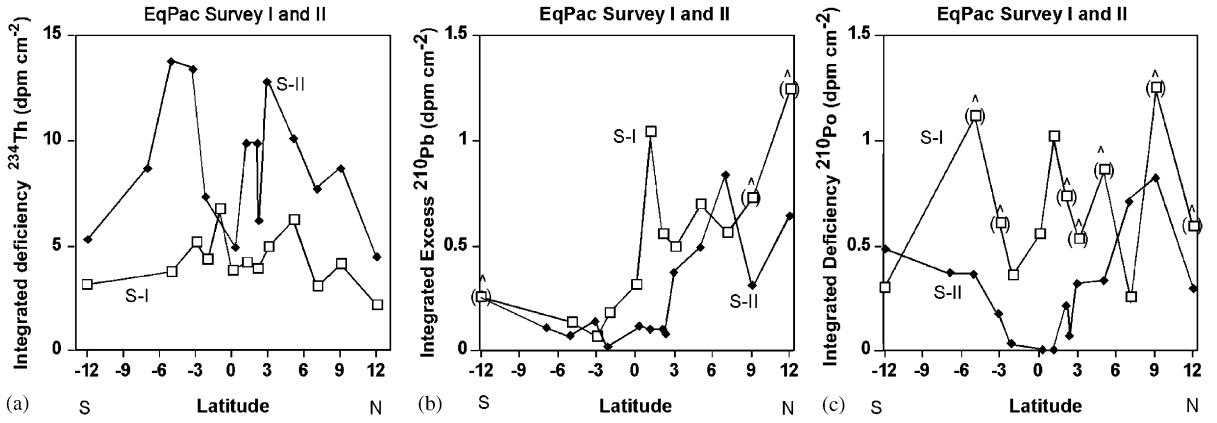

Fig. 3. Inventories (dpm cm^{-2}) of integrated: (a) ^{234}Th deficiency relative to ^{238}U, (b) excess ^{210}Pb relative to ^{226}Ra, (c) ^{210}Po deficiency relative to ^{210}Pb from 0 to 250 m from 12°N to 12°S along 140°W for EqPac Survey I (□) and Survey II (◇). Values in parentheses are minimum values indicating that the deficiency in the water column extended deeper than our sampling.

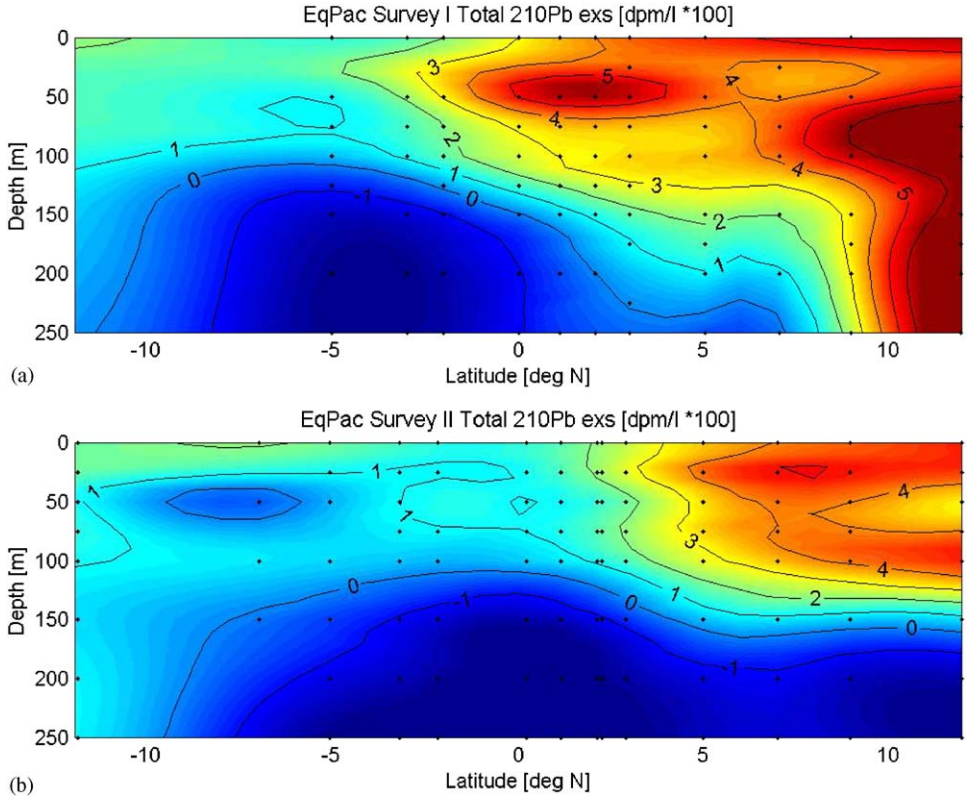

Fig. 4. Meridional section of the ^{210}Pb excess (dpm l^{-1}) for 0–250 m from 12°N to 12°S at 140°W: (a) Survey I; (b) Survey II.

possibly because of reduced upwelling. Values in parentheses represent lower limits as the excess ^{210}Pb extended deeper than our sampling (>250 m) at those stations. Nozaki et al. (1990) determined integrated ^{210}Pb as large as 10 dpm m^{-2} in the Okinawa Trough. Our values at 140°W are much lower (<1.3 dpm m^{-2}) because of the remoteness of these transects from continental sources of ^{222}Rn.

The total ^{210}Po deficiency (defined as ^{210}Po$_{def}$ = ^{210}Pb–^{210}Po) had a much more bimodal and symmetrical pattern about the equator than either ^{234}Th$_{def}$ or ^{210}Pb$_{exs}$ (Fig. 5) and frequently extended to depths greater than 200 m. The general meridional patterns were similar for both Survey I and Survey II, but the integrated values showed striking differences between these periods (Fig. 3c). During Survey I (El Nino) the integrated deficiencies were much larger (about 1 dpm m^{-2}) and showed no discernible meridional trend (note however that many points are lower limits because the water column deficiencies extended deeper than we sampled). During Survey II (cold tongue) ^{210}Po$_{def}$ was very low at the equator (<0.05 dpm m^{-2}) and increased to the north and south. Even though new production was larger during Survey II, the upwelled flux of water with small ^{210}Po deficiencies probably dominated the mass balance.

The University of Washington (UW)-MLML intercalibrations for stable Pb were conducted on samples from EqPac Time Series I at the equator (Fig. 6a), Time Series II at the equator (Fig. 6b) and Time Series II at 12°S (Fig. 6c). The agreement was excellent and UW Pb = 1.08 MLML Pb −9.3. with $r^2 = 0.86$. Stable Pb generally was higher at

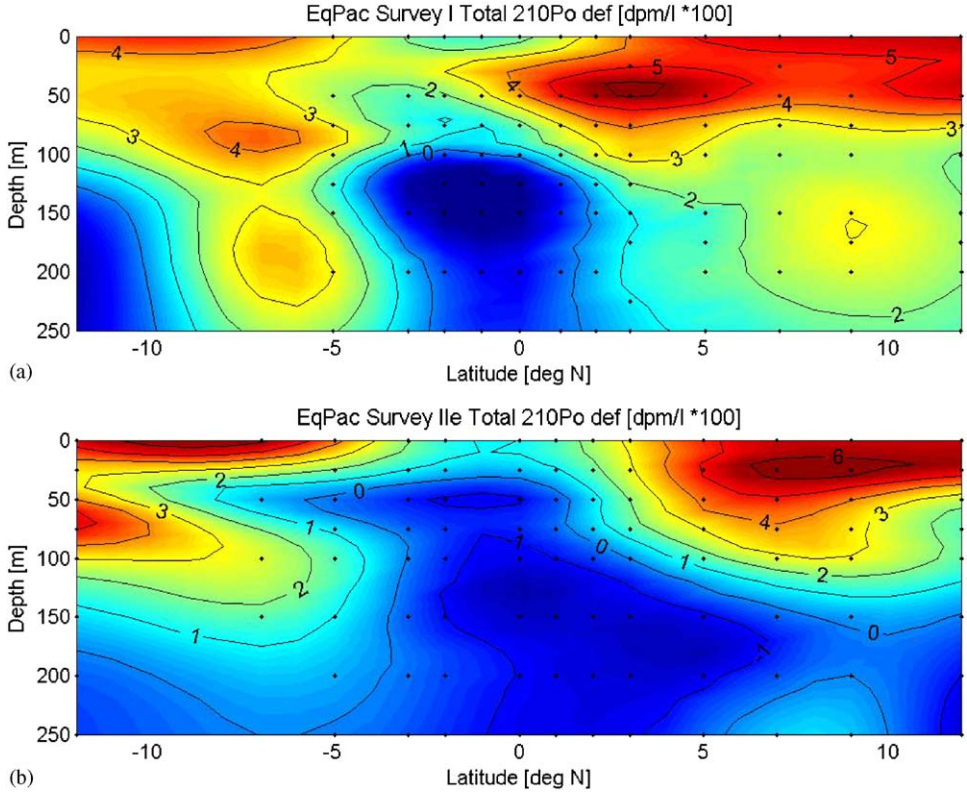

Fig. 5. Meridional section of the ^{210}Po deficiency (dpm l^{-1}) for 0 to 250 m from 12°N to 12°S at 140°W: (a) Survey I; (b) Survey II.

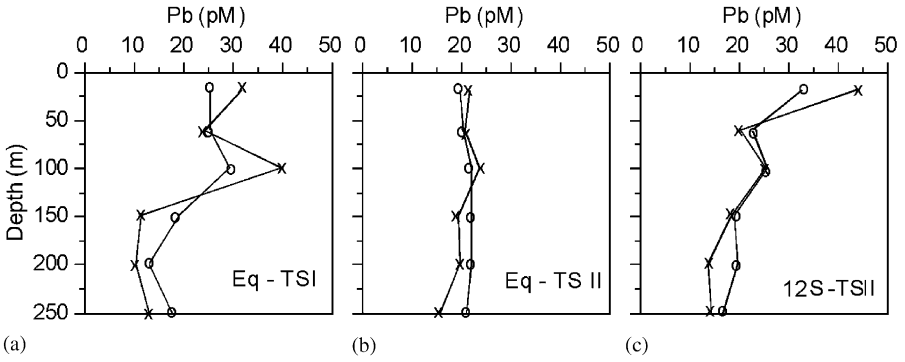

Fig. 6. Interlaboratory comparison of Pb analyses: (a) EqPac Time Series I (Eq; 140°W); (b) EqPac Time Series II (Eq; 140°W), (c) EqPac Time Series II (12°S; 140°W). Circles (○) by graphite furnace atomic absorption spectrophotometry Moss Landing Marine Lab (MLML). Crosses (×) by flow injection-inductively coupled plasma mass spectrometry at University of Washington (UW).

the surface (about 20–44 pM) and decreased with depth to about 15 pM at 250 m. The vertical profiles of lead for Survey I and Survey II (as well as the data from Time Series I and II at the equator) are shown in Fig. 7. There was no decrease in surface Pb from 12°N to 12°S at 140°W, contrary to the decrease observed by Flegal and Patterson (1983) at 160°W.

4. Discussion

4.1. Particulate fractionation of ^{234}Th, ^{210}Pb and ^{210}Po

^{234}Th, ^{210}Pb and ^{210}Po are all particle reactive, yet they partition differently between particle types. For example, ^{210}Po is generally deficient relative to ^{210}Pb in surface waters because of its stronger affinity for all exported particles and its concentration by phytoplankton (Shannon et al., 1970; Heyraud and Cherry, 1979). ^{234}Th and ^{210}Pb may be removed by sorption on the surfaces of all particles (e.g., Nozaki et al., 1976; Nozaki and Tsunogai, 1976; Murray et al., 1989), but ^{210}Po has a more nutrient like behavior and is taken up by the interior of cells (Fisher et al., 1983).

Because ^{210}Pb and ^{210}Po have different scavenging pathways it is useful to look at the ^{210}Po/^{210}Pb ratio in different phases. Dissolved ^{210}Po/^{210}Pb (Fig. 8a) is similar to total ^{210}Po/^{210}Pb (Fig. 1c) in that, in both cases, there is a deficiency of ^{210}Po relative to ^{210}Pb in the surface layer. ^{210}Po is in excess relative to ^{210}Pb in suspended particles (Fig. 8b) with most ^{210}Po/^{210}Pb ratios less than 25, except for one high value at 45. The ratios of ^{210}Po/^{210}Pb in trap samples (Fig. 8c) are the same or higher with some values reaching as high as 55. The large enrichments of ^{210}Po relative to ^{210}Pb in particulate phases are probably due to preferential uptake of ^{210}Po by plankton.

The contrasting behavior of ^{234}Th, ^{210}Pb and ^{210}Po can be assessed quantitatively through the particulate/dissolved distribution coefficients and fractionation factors (F) for these nuclides. The distribution coefficient (K_d) is defined as

$$K_d = \frac{C_p/C_d}{\mathrm{TSM}}, \quad (3)$$

where C_p and C_d are concentrations of the nuclides in particulate and dissolved forms and TSM is the TSM concentration. The values of these K_ds in the equatorial Pacific are similar to those from other regions (e.g., the New England shelf and slope, Bacon et al., 1988). Log K_d (Th) is about 7 and does not vary with depth. Log K_d (Pb) increases with depth from 5 at the surface to 6 at 250 m.

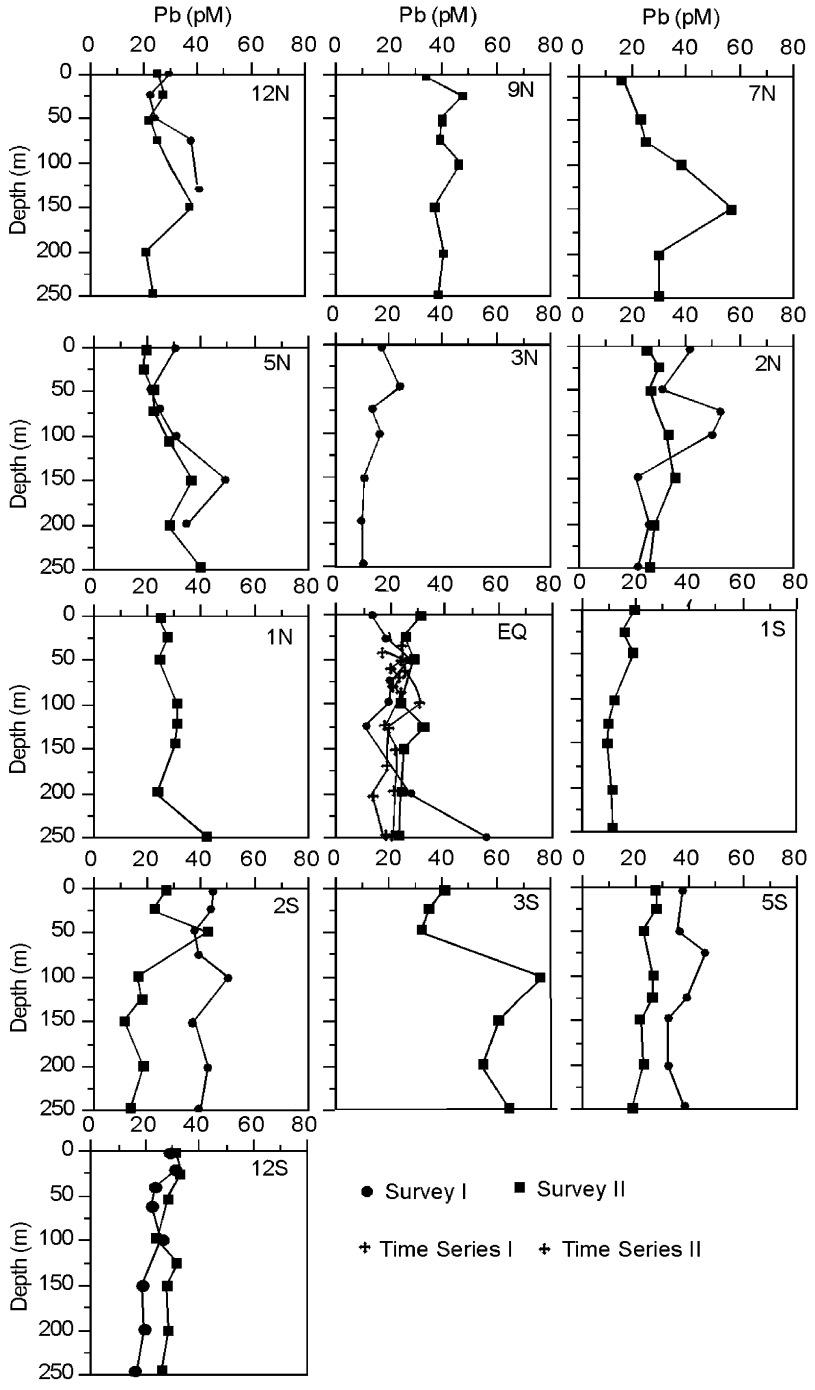

Fig. 7. Vertical profiles of total dissolvable stable lead concentrations for EqPac Survey I (□) and Survey II (●) from 12°N to 12°S. Values by Moss Landing Marine Labs (MLML) at the equator and 12S for TS I (×) and TS II (+) are also shown.

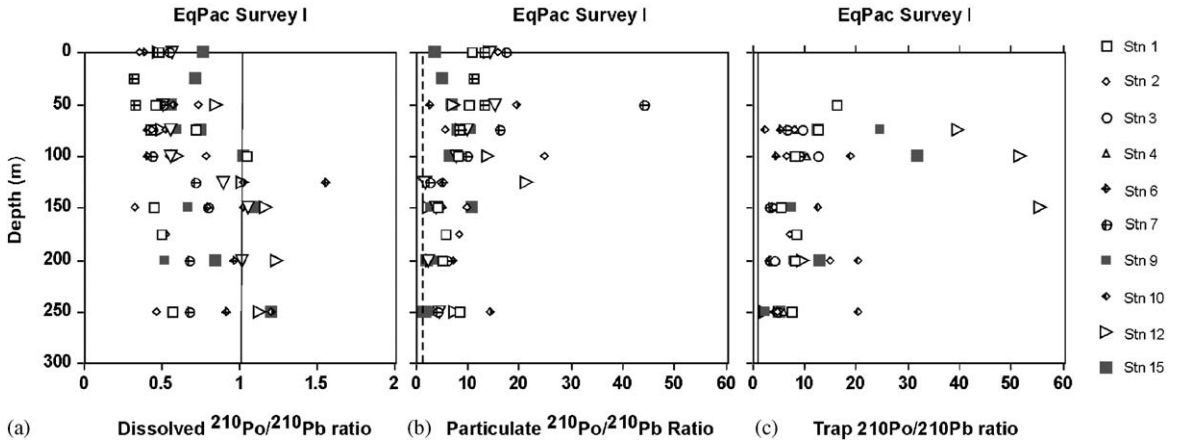

Fig. 8. $^{210}Po/^{210}Pb$ in the (a) dissolved phase, (b) suspended particles (>0.45 μm Millipore), (c) PIT sediment trap particles for Survey I for 0–250 m along 12°N to 12°S at 140°W.

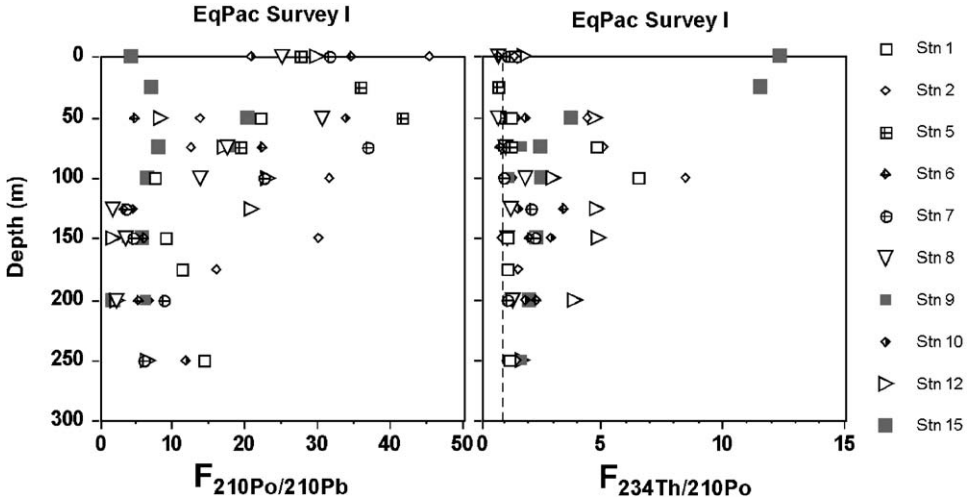

Fig. 9. Fractionation of (a) ^{210}Po relative to ^{210}Pb and (b) ^{234}Th relative to ^{210}Po in suspended particles for EqPac Survey I. The affinity (F) is expressed as the ratio of the distribution coefficients. A vertical dotted line is drawn for a ratio of one.

Log K_d (Po) increases slightly with depth from 6.5 at the surface to 7 at 250 m. Otherwise, there is no temporal or spatial variability in these values. These values for ^{234}Th are significantly higher than K_d values determined for clean inorganic surfaces (e.g. $CaCO_3$, SiO_2, FeOOH, MnO_2) in seawater but are similar to K_d values for acid polysaccharides (APS) (Guo et al., 2002; Quigley et al., 2002). This comparison has been used to argue that the surface chemistry of ocean particles is determined by sorbed APS.

The fractionation factors (F) are the ratios of the distribution coefficients, e.g.,

$$F_{\mathrm{Po/Pb}} = \frac{K_{\mathrm{d}}(\mathrm{Po})}{K_{\mathrm{d}}(\mathrm{Pb})}, \tag{4}$$

when calculating the values of F, the values of TSM cancel. In this data set, $F_{\mathrm{Po/Pb}}$ are all greater than 1 and range up to 45 (Fig. 9a). There is a general tendency for the particulate preference for Po to be larger in the upper 100 m than deeper than 100 m, which is consistent with the preferential uptake of ^{210}Po by plankton. Bacon et al. (1988) observed a minimum in $F_{\mathrm{Po/Pb}}$ in the subsurface zone (~100 m) of the mid-Atlantic Bight due to ^{210}Po remineralization. This feature was not observed in our data, perhaps because we did not sample deep enough.

$F_{\mathrm{Th/Po}}$ is also greater than 1 (Fig. 9b) but has a different distribution versus depth than $F_{\mathrm{Po/Pb}}$ with a maximum centered at about 100 m. Comparison of these fractionation factors indicates an overall selectivity for particles of $^{234}\mathrm{Th} > ^{210}\mathrm{Po} > ^{210}\mathrm{Pb}$. This sequence is different from the order observed in experimental studies with plankton ($^{210}\mathrm{Po} \gg ^{210}\mathrm{Pb} = ^{234}\mathrm{Th}$), probably because natural particle assemblages in the equatorial Pacific consist of detritus and inorganic material as well as plankton (Dunne et al., 1997).

Dunne et al (1997) demonstrated that phytoplankton played only a minor role in ^{234}Th scavenging because of rapid recycling in the microbial loop. Applying these results to ^{210}Po suggests that it's preferential scavenging by phytoplankton would be effectively short-circuited by grazing even more than for ^{234}Th, consistent with observed fractionation factors.

4.2. Scavenging residence times for dissolved ^{234}Th, ^{210}Pb and ^{210}Po

For ^{234}Th, ^{210}Pb and ^{210}Po the general form of the mass balance equations between sources and sinks (all in dpm m^{-2} d^{-1}) are

$$\frac{\partial A_{^{234}\mathrm{Th}}}{\partial t} = A_{^{238}\mathrm{U}}\lambda_{^{234}\mathrm{Th}} - A_{^{234}\mathrm{Th}}\lambda_{^{234}\mathrm{Th}} - P - V(\mathrm{adv} + \mathrm{diff\ transport}), \tag{5}$$

$$\frac{\partial A_{^{210}\mathrm{Pb}}}{\partial t} = A_{^{226}\mathrm{Ra}}\lambda_{^{210}\mathrm{Pb}} - A_{^{210}\mathrm{Pb}}\lambda_{^{210}\mathrm{Pb}} + I_{^{210}\mathrm{Pb}} - P - V(\mathrm{adv} + \mathrm{diff\ transport}), \tag{6}$$

$$\frac{\partial A_{^{210}\mathrm{Po}}}{\partial t} = A_{^{210}\mathrm{Pb}}\lambda_{^{210}\mathrm{Po}} - A_{^{210}\mathrm{Po}}\lambda_{^{210}\mathrm{Po}} - P - V(\mathrm{adv} + \mathrm{diff\ transport}). \tag{7}$$

In these equations, $\partial/\partial t$ is the time rate of change, the activities (A) are defined as dpm m^{-2}, λ is the decay constant (d^{-1}), $I_{^{210}\mathrm{Pb}}$ is the ^{210}Pb input from the atmosphere, P is the scavenging removal rate or export flux and V is the sum of the three dimensional advective and diffusive fluxes.

Scavenging residence times are based on dissolved concentrations, and reflect the rate of dissolved to particulate transformation. For calculating scavenging residence times from the euphotic zone, the scavenging removal rates (P) are expressed as $\Psi\mathrm{Ai}$, where Ψ is the scavenging removal rate constant (d^{-1}) and Ai is the integrated activity of dissolved isotopes (dpm m^{-2} to 120 m). The time rate of change is difficult to evaluate with only two data sets separated by 6 months. Bacon et al. (1996) used the EqPac time-series data sets to argue that steady state could be assumed for ^{234}Th with minimal error. Assuming steady state and that upwelling (w) and meridional (v) advection are the only necessary transport terms we get

$$\mathrm{Ai}_{^{238}\mathrm{U}}\lambda_{^{234}\mathrm{Th}} = \mathrm{Ai}_{^{234}\mathrm{Th}}\lambda_{^{234}\mathrm{Th}} + \Psi_{^{234}\mathrm{Th}}\mathrm{Ai}_{^{234}\mathrm{Th}} - w\frac{\partial \mathrm{Ai}_{^{234}\mathrm{Th}}}{\partial z} + v\frac{\partial \mathrm{Ai}_{^{234}\mathrm{Th}}}{\partial y}, \tag{8}$$

$$I_{^{210}\mathrm{Pb}} + \mathrm{Ai}_{^{226}\mathrm{Ra}}\lambda_{^{210}\mathrm{Pb}} = \mathrm{Ai}_{^{210}\mathrm{Pb}}\lambda_{^{210}\mathrm{Pb}} + \Psi_{^{210}\mathrm{Pb}}\mathrm{Ai}_{^{210}\mathrm{Pb}}w\frac{\partial A_{^{210}\mathrm{Pb}}}{\partial z} + v\frac{\partial A_{^{210}\mathrm{Pb}}}{\partial y}, \tag{9}$$

$$\mathrm{Ai}_{^{210}\mathrm{Pb}}\lambda_{^{210}\mathrm{Po}} = \mathrm{Ai}_{^{210}\mathrm{Po}}\lambda_{^{210}\mathrm{Po}} + \Psi_{^{210}\mathrm{Po}}\mathrm{Ai}_{^{210}\mathrm{Po}} - w\frac{\partial \mathrm{Ai}_{^{210}\mathrm{Po}}}{\partial z} + v\frac{\partial \mathrm{Ai}_{^{210}\mathrm{Po}}}{\partial y}. \tag{10}$$

For these calculations, the magnitude of w and v were taken from Chai (1995) as described by Buesseler et al. (1995), Murray et al. (1996) and Bacon et al. (1996). The contoured streamlines of these velocities were shown in Dunne and Murray

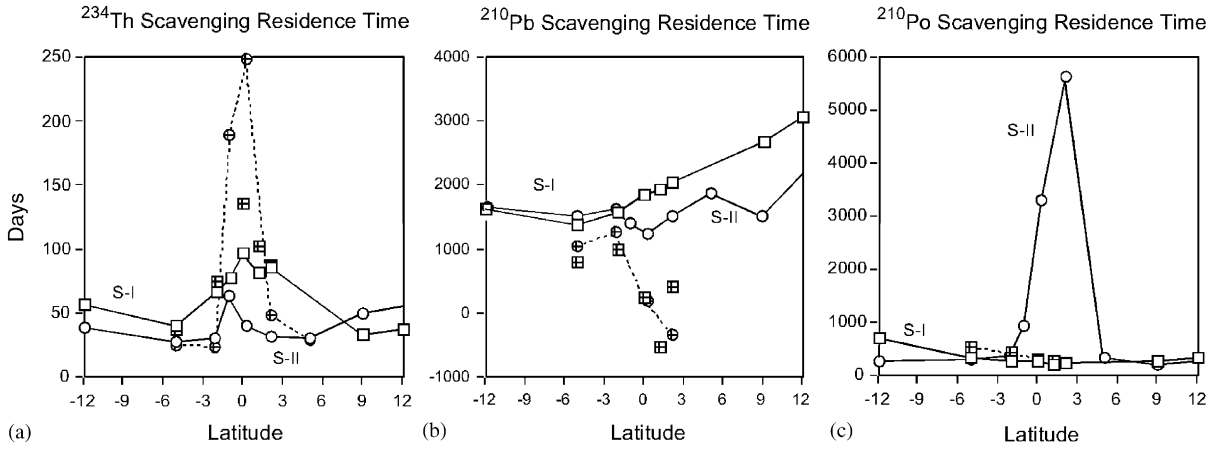

Fig. 10. Scavenging residence times using the integrated activities from 0 to 120 m of dissolved (a) ^{234}Th, (b) ^{210}Pb and (c) ^{210}Po for 12°N to 12°S at 140°W. The symbols represent Survey I (□) and Survey II (○). Points from 5°N to 5°S connected by dashed lines include advection corrections.

(1999). The advection corrections were only applied between 5°N and 5°S where the velocities from Chai (1995) are available. The assumption to neglect zonal advection was acceptable for ^{234}Th (e.g. Buesseler et al., 1995) but is impossible to evaluate explicitly here for ^{210}Pb and ^{210}Po because of the lack of data in the zonal direction. It is unlikely that the zonal gradients are large enough for this term to be important here. The residence times are expressed as $\tau_i = \psi_i^{-1}$ and are calculated as follows from Eqs. (11) to (13), with the transport terms expressed as $V(= -w(\partial \mathrm{Ai})/\partial z + v(\partial \mathrm{Ai})/\partial y)$:

$$\tau_{^{234}\mathrm{Th}} = \frac{A_{^{234}\mathrm{Th}}}{(A_{^{238}\mathrm{U}} - A_{^{234}\mathrm{Th}})\lambda_{^{234}\mathrm{Th}} - V}, \quad (11)$$

$$\tau_{^{210}\mathrm{Pb}} = \frac{A_{^{210}\mathrm{Pb}}}{I_{^{210}\mathrm{Pb}} + (A_{^{226}\mathrm{Ra}} - A_{^{210}\mathrm{Pb}})\lambda_{^{210}\mathrm{Pb}} - V}, \quad (12)$$

$$\tau_{^{210}\mathrm{Po}} = \frac{A_{^{210}\mathrm{P0}}}{(A_{^{210}\mathrm{Pb}} - A_{^{210}\mathrm{Po}})\lambda_{^{210}\mathrm{Po}} - V}. \quad (13)$$

The results are shown in Fig. 10 with and without the advection terms included. A larger magnitude of V results in a larger value of τ, but V itself consists of two terms, each with an advection velocity and a concentration gradient, which have opposite effects. Thus, the effect of the transport corrections is not easy to predict. $\tau_{^{234}\mathrm{Th}}$ ranged from 25 to 250 d and were longer for Survey I than Survey II, except right at the equator where transport dominates (Fig. 10a). For both surveys τ was longer near the equator than to the north and south, as shown previously by Dunne et al. (1997). The shorter values of $\tau_{^{234}\mathrm{Th}}$ during Survey II have been explained as due to increased export production at that time (Murray et al., 1996). Coale and Bruland (1985) and Bruland and Coale (1986) showed an inverse relationship between ψ_{Th} and primary and new production. With advection corrections, τ was longer at the equator during Survey II because of the larger horizontal advection transport at that time.

$\tau_{^{210}\mathrm{Pb}}$ ranged from 1500 to 3000 d (4–8 years) and increased in the northern hemisphere in these surveys (Fig. 10b). A constant atmospheric input of 0.25 dpm cm^{-2} year^{-1} was included in the mass balance because Turekian et al. (1989) showed that atmospheric ^{210}Pb fluxes at widely separated points in the mid-Pacific basin are all in the range 0.2–0.3 dpm m^{-2} year^{-1}. Our own calculations in the next section support this choice. North of the equator, $\tau_{^{210}\mathrm{Pb}}$ was lower during Survey II than Survey I. Including the advection terms decreased

the value of $\tau_{^{210}Pb}$ to 200–1000 d, especially at the equator to 2°N because of the dominance of the upwelling term in these calculations. Nozaki et al. (1990) used a similar approach for the Okinawa Trough. Because their site was closer to Asia they used a larger atmospheric input of $I_{^{210}Pb} = 2\,dpm\,cm^{-2}$. They calculated a mean ^{210}Pb residence time of ~2 years. Sarin et al. (1999) calculated $\tau_{^{210}Pb}$ of 400–780 d (1.1–2.1 years) in the central Atlantic. Bacon et al. (1976) and Nozaki et al. (1997) both calculated $\tau_{^{210}Pb} = 2.5$ years, for the North Atlantic and western equatorial Pacific, respectively.

$\tau_{^{210}Po}$ are mostly in the range 100–500 d and show little meridional pattern except from 1°S to 2°N during Survey II, where they increased to over 5000 d (Fig. 10c). These long $\tau_{^{210}Po}$ are clearly anomalous and were eliminated when advection corrections are made. Sarin et al. (1999) calculated $\tau_{^{210}Po}$ of 73–130 d in the central Atlantic. Bacon et al. (1976) calculated $\tau_{^{210}Po}$ of 219 d for the North Atlantic. Shimmield et al. (1995) calculated $\tau_{^{210}Po}$ of 73 d to 1.0 year. Nozaki et al. (1997) calculated τ_{Po} of 140 d to 2.5 years for the western tropical Pacific and also found a positive correlation between the scavenging rate constant and chlorophyll-*a*.

4.3. Atmospheric input of ^{210}Pb

The surface waters of the tropical Pacific have excess ^{210}Pb, which increases sharply north of the equator (Fig. 3b, 4). The origin of this excess ^{210}Pb is decay of atmospheric ^{222}Rn ($t_{1/2} = 3.8$ d), which emanates from continental rocks and is transported over the oceans. (Turekian et al., 1989). When $^{210}Pb_{atm}$ is produced, it is scavenged rather quickly by precipitation and dry fallout. Its mean life with respect to removal from the atmosphere is about 5–15 d (Turekian et al., 1977; Balkanski et al., 1993; Hussain et al., 1998). Because this excess ^{210}Pb is produced at the Earth's surface, it may be an analogue for other natural (e.g. Fe) and anthropogenic (e.g. stable Pb) components injected into the troposphere from the continents (Turekian and Cochran, 1981; Kim et al., 1999). However, Balkanski et al. (1993) argued that ^{210}Pb should not be viewed as a generic tracer of continental aerosols.

A number of different techniques have been used to measure ^{210}Pb deposition fluxes in the Pacific (Turekian et al., 1989). As most measurement techniques use soil or bucket samples, they are limited to land sites. The pattern of deposition in the North Pacific displays high values (0.5–2.5 $dpm\,cm^{-2}\,year^{-1}$) in Japan with fluxes decreasing with distance from the Asian source to relatively constant values in the range of 0.2–0.3 $dpm\,cm^{-2}\,year^{-1}$ across the Pacific from Enewetak to Fanning Island to Los Angeles, CA. Fanning Island (5°N; 160°W) is the site closest to our study area (140°W).

The mean values of ^{210}Pb concentration in air generally decrease from north to south (Turekian et al., 1989). The concentrations of ^{210}Pb in air over the South Pacific are roughly half those over the North Pacific reflecting the smaller ratio of land to ocean in the Southern Hemisphere and aerosol washout associated with the Intertropical Convergence Zone (ITCZ). The ITCZ is a well-defined, narrow but effective rain fall barrier to southward transport of northern hemisphere dust in the central equatorial Pacific (Rea, 1994). It is located north of the equator because the shallowness of the thermocline in the eastern equatorial Pacific and the geometries of the continents, which determine the large-scale wind patterns (Philander et al., 1996). Temporal variations in atmospheric ^{210}Pb concentrations are controlled by variability in air mass trajectory and rainfall.

Because previous measurements were limited to land sites, we used an approach of estimating the atmospheric source of ^{210}Pb for our tropical ocean site at 140°W by combining the water column and sediment trap data sets. The steady-state mass balance for ^{210}Pb in the surface ocean was given in Eq. (6). We know $A_{^{226}Ra}$ and $A_{^{210}Pb}$ (both in integrated values of $dpm\,cm^{-2}$). By assuming that the flux measured by the sediment traps at 120 m equals the scavenging removal and we can calculate the atmospheric input ($I_{^{210}Pb}$) at each station.

The atmospheric input of ^{210}Pb calculated by this approach is shown in Fig. 11. Most values are between 0.1 and 0.5 $dpm\,cm^{-2}\,year^{-1}$. The average

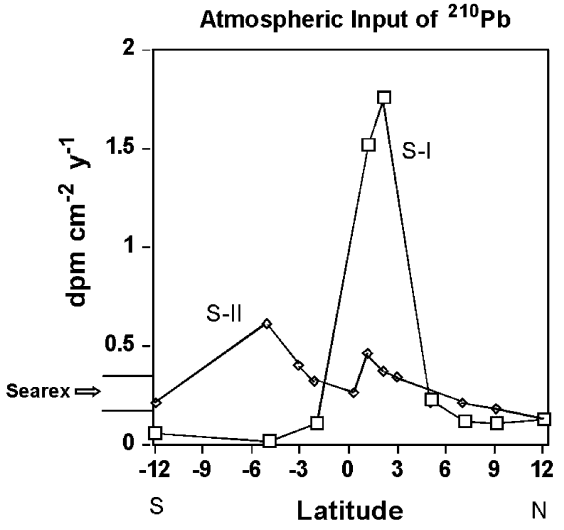

Fig. 11. Atmospheric input of ^{210}Pb (dpm cm^{-2} year^{-1}) for Survey I (□) and Survey II (◇) along 12°N to 12°S at 140°W. The horizontal lines on the left represent the upper and lower limits and the mean values determined during Searex by Turekian et al. (1989).

values for Survey I (omitting the high points at 2°N and 3°N) and Survey II are 0.12 and 0.32 dpm cm^{-2} year^{-1}, respectively. The grand average of 0.25 dpm cm^{-2} year^{-1} is in good agreement with the range of values measured from Enewetak to Fanning to Los Angeles, CA by Turekian et al. (1989) during the Searex Program.

The expected meridional pattern of an increase north of the equator was not observed. However, there was a strong maximum in atmospheric input of ^{210}Pb at 2–3°N during Survey I. This was the location of the ITCZ at that time, which corresponded to weak El Nino conditions (Murray et al., 1994). In addition, the ^{210}Pb deposition south of the equator was lower than that to the north, suggesting that precipitation associated with the ITCZ cleansed the atmosphere of ^{210}Pb during Survey I. There was no equivalent maximum during Survey II, consistent with the fact that there was no well-developed ITCZ zone established at that time.

The situation of high atmospheric deposition of ^{210}Pb under the ITCZ suggests a strong preference of wet-deposition over dry deposition. Would the same be true of iron? For most of this EqPac region the trade winds come from Central America. Any iron associated with Asian dust input to the North Pacific would likely be washed out by the ITCZ before it reached the equator. Data are needed to determine the relationship between Fe and ^{210}Pb in atmospheric deposition in this region.

4.4. Atmospheric input of stable Pb

Atmospheric deposition supplies most of the Pb in the ocean surface mixed layer and thermocline (Maring et al., 1989). Today most of this lead is anthropogenic. Thus, Pb concentrations in the surface ocean are not at steady state and exhibit temporal variability (Véron et al., 1993). The atmospheric flux of Pb increased steadily during the industrial revolution (Murozumi et al., 1969; Shotyk et al., 1998) but increased more rapidly from 1930 to 1970 because of the use of alkyl leaded gasolines (Boyle et al., 1986). From 1970 to the present the source of Pb from gasoline decreased dramatically (Nriagu, 1989; Bollhöfer and Rosman, 2001)). Because the source of this Pb is the industrialized continents in the northern hemisphere, higher oceanic concentrations are found there.

Schaule and Patterson (1983) demonstrated that there was a large anthropogenic Pb signal in the western North Atlantic. Boyle et al. (1986), Shen and Boyle (1988) and Boyle et al. (1994) have shown that lead concentrations are highly variable in the surface water of the North Atlantic. Normalization of stable Pb to ^{210}Pb minimizes this variability because ^{210}Pb and Pb sources from North America are spatially correlated and ^{210}Pb sources are constant. Because anthropogenic sources have declined, the Pb/^{210}Pb ratio in surface waters from Bermuda has steadily declined since at least 1980 (Boyle et al., 1994).

There have been few determinations of Pb in seawater or the atmospheric flux of Pb in the Pacific (Table 1). Schaule and Patterson (1981) measured Pb in 34 surface- and deep-samples in the northeast Pacific. Pb concentrations increased from 5 to 15 ng kg^{-1} (~25–75 pmol kg^{-1}) along a transect from the California coast to the center of the North Pacific Gyre. They used sediment data

Table 1
Estimates of the atmospheric flux of stable lead to the ocean

Location	Flux (pmol cm^{-2} $year^{-1}$)	Time period	Reference
NE Pacific	14	Pre-industrial	Schaule and Patterson (1981)
Sierra Nevada, CA	24	Pre-industrial	Patterson and Settle (1987)
North Pacific	289	1980s	Patterson and Settle (1987)
North Pacific			
Easterlies	29	1980s	Flegal and Patterson (1983)
Westerlies	241	1980s	Flegal and Patterson (1983)
North Pacific	72	May–June 1986	Maring et al. (1989)
Central Tropical Pacific (140°W; 12°N to 12°S).	140–110	1992	This study

to estimate the historical pre-industrial flux to sediments during the Pleistocene (~3 ng cm^{-2} $year^{-1}$ or 14 pmol cm^{-2} $year^{-1}$). The isotopic signature of Pb in sediments suggests that wind-blown loess from Asia dominated pre-industrial Pb input to much of the North Pacific (Jones et al., 2000). Samples from south of the ITCZ (~5°N) have a smaller loess concentration relative to inputs from volcanic ash and young crustal rocks around the Pacific Rim. The prehistoric flux to the Sierra Nevada was about 5 ng cm^{-2} $year^{-1}$ (or 24 pmol cm^{-2} $year^{-1}$)(Patterson and Settle, 1987). The eolian flux for the 1980s to the North Pacific was estimated from three independent approaches to be about 60 ng cm^{-2} $year^{-1}$ (or 289 pmol cm^{-2} $year^{-1}$). Flegal and Patterson (1983) measured Pb along a surface transect and at two vertical profiles in the Pacific at 14°N and 20°S at 160°W. Surface Pb decreased from 11 ng kg^{-1} (~53 pmol kg^{-1}) at 14°N to 2.5 ng kg^{-1} (~12 pmol kg^{-1}) at 20°S. Eolian lead input fluxes were estimated to be ~6 ng cm^{-2} $year^{-1}$ (~29 pmol cm^{-2} $year^{-1}$) and 50 ng cm^{-2} $year^{-1}$ (~241 pmol cm^{-2} $year^{-1}$) in the North Pacific easterlies and westerlies, respectively. Measurements by Maring et al. (1989) of four rain samples from 40–45°N resulted in a lower atmospheric flux of 15 ng cm^{-2} $year^{-1}$ (72 pmol cm^{-2} $year^{-1}$) in May–June 1986.

The EqPac data for Pb and ^{210}Pb were combined to estimate the atmospheric input of stable Pb from 12°N to 12°S along 140°W during Survey I and II. In this approach, the steady state mass balance equations for ^{210}Pb and Pb are combined. The mass balance for ^{210}Pb was given in Eq. (6). The steady-state mass balance for stable lead is

$$I_{Pb} = \Psi_{Pb}[Pb]. \tag{14}$$

For ^{210}Pb the atmospheric input and production from ^{226}Ra are balanced by decay and first-order scavenging. For stable Pb, the balance is between atmospheric input and first order scavenging. Even though stable Pb is a transient tracer we can assume steady state in this case as the time scales of these processes are shorter than the rate of change in the atmospheric flux. We assume that the first-order scavenging rate constants for Pb and ^{210}Pb are equal. Thus,

$$\Psi_{^{210}Pb} = \Psi_{Pb} \tag{15}$$

with this assumption the two mass balance equations (Eqs. (6) and (14)) can be combined and solved for the ratio of [Pb] to ^{210}Pb, thus,

$$\frac{[Pb]}{A_{^{210}Pb}} = \frac{I_{Pb}(\lambda_{^{210}Pb} + \Psi_{^{210}Pb})}{\Psi_{Pb}(I_{^{210}Pb} + A_{^{226}Ra})}. \tag{16}$$

The vertical profiles of the ratio of Pb to ^{210}Pb from 12°N to 12°S at 140°W are plotted in Fig. 12. The ratios for Survey I and II ranged from 100 to 600 pmol dpm^{-1}, with an average value of 298 pmol dpm^{-1} for Survey I and 329 pmol dpm^{-1} for Survey II. The same ratio at Bermuda decreased from 1000 pmol dpm^{-1} in 1980 to 400 pmol dpm^{-1} in 1988 (Boyle et al., 1994).

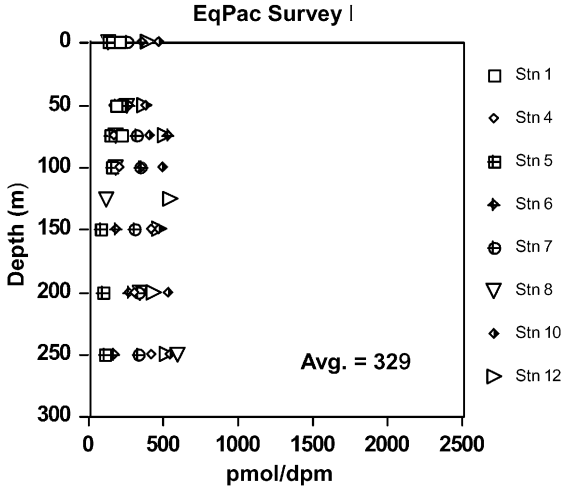

Fig. 12. Ratio of stable Pb to ^{210}Pb (pmol/dpm) for EqPac Survey I for 0–250 m from 12°N to 12°S at 140°W.

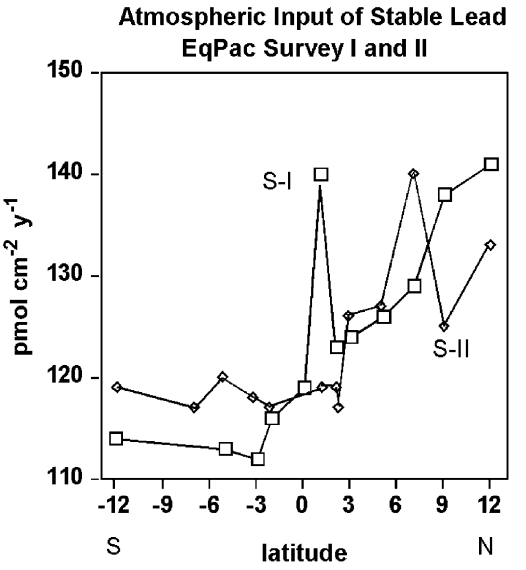

Fig. 13. Atmospheric input of stable Pb (pmol cm^{-2} year^{-1}) for EqPac Survey I (□) and Survey II (◇) from 12°N to 12°S at 140°W.

Assuming that $I_{^{210}Pb} = 0.25$ dpm cm^{-2} y^{-1} (from Fig. 11) and Pb/$A_{^{210}Pb} = 298$ pmol dpm^{-1} for Survey I and 329 pmol dpm^{-1} for Survey II, we calculated the atmospheric input of stable Pb. The values used for $\Psi_{^{210}Pb}$ were calculated from the residence time results of ^{210}Pb in Fig. 10b.

The resulting atmospheric input of stable Pb ranged from $I_{Pb} = 110-140$ pmol cm^{-2} year^{-1} (Fig. 13). The atmospheric flux is low in the southern hemisphere and increases steadily north of the equator. The highest values of 140 pmol cm^{-2} year^{-1} are at 12°N. These are lower than the earlier measurements by Patterson and Settle (1987) and Flegal and Patterson (1983), which would be consistent with decreasing atmospheric fluxes over the past 20 years, but higher than those measured on a single cruise by Maring et al. (1989). The uncertainty in our fluxes is probably ±15% based on propagation of errors using average values for the stable Pb/$A_{^{210}Pb}$ ratio and atmospheric input of ^{210}Pb.

4.5. A method for estimating carbon export fluxes using ^{210}Po

Several studies have explored the use of ^{234}Th as a tracer for the export flux of particulate matter from the euphotic zone (e.g., Buesseler et al, 1992, 1995; Murray et al., 1996; Bacon et al., 1996; Kim and Church, 2001). The approach is to calculate the export flux of ^{234}Th from its deficiency in the water column then convert the ^{234}Th flux to that for carbon (or nitrogen or other elements) by measuring the C/^{234}Th ratio in sinking particles. When sediment traps are used to obtain the sinking particles, as we did in this study, this is the same as using ^{234}Th as a tracer for correcting the carbon flux for trap bias. The fluxes calculated by this approach integrate over the mean life of ^{234}Th due to both decay and scavenging ($= 1/\lambda + \psi$) (~30 d).

Previous work in the Bering Sea by Nozaki et al. (1998) showed that the $^{210}Po_{def}$ can extend to depths greater than 1000 m and reach values of 2.6–4.3 dpm m^{-2}. Values in the Okinawa Trough reached 8 dpm m^{-2} (Nozaki et al., 1990). The low values in the equatorial Pacific (<1.3 dpm m^{-2}) are probably due to low new production (e.g. McCarthy et al., 1996; Aufdenkampe et al., 2001). It has been argued that because ^{210}Po is taken up by the interior of cells, in contrast to ^{234}Th, which

is adsorbed by all particle surfaces, ^{210}Po may be a better tracer for organic carbon than ^{234}Th. Because ^{210}Po has a half-life of 138 d, it would integrate the export fluxes over a longer period of time.

There have been few comparable studies. Shimmield et al. (1995) used ^{210}Po to estimate POC export flux in the Bellinghausen Sea by dividing the POC inventory by the estimated residence time of particulate ^{210}Po. In that study, the ^{210}Po-based estimates of flux (2.2 mmol C m^{-2} d^{-1}) were about 10 times less than the ^{234}Th based estimates (21 mmol C m^{-2} d^{-1}). Their calculations of ^{210}Po and ^{234}Th flux did not include upwelling and lateral transport. They suggested that the ^{234}Th flux was enhanced because of ice-rafted lithogenic material. Friederich and Rutgers van der Loeff (2002) used multiple regression equations to determine the relationships of ^{234}Th, ^{210}Pb and ^{210}Po to POC and biogenic silica (BSi). These regressions were combined with the radionuclide export fluxes to calculate the export flux of POC and BSi. The results showed a preference of ^{210}Po for POC and of ^{210}Pb for biogenic silica.

Here we evaluate the use of ^{210}Po to calculate particulate carbon export. First we calculate the export fluxes of ^{210}Po from water column profiles of total ^{210}Po using the mass balance for ^{210}Po (Eq. (7)) where A is the activity of total ^{210}Po and ^{210}Pb, and P is the particulate export flux of ^{210}Po. Assuming steady state and that upwelling (w) and meridional (v) advection are the only necessary transport terms we get

$$P = (A_{^{210}\mathrm{Pb}} - A_{^{210}\mathrm{Po}})\lambda_{^{210}\mathrm{Po}} + w\frac{\delta A_{^{210}\mathrm{Po}}}{\delta z} - v\frac{\delta A_{^{210}\mathrm{Po}}}{\delta y}. \quad (17)$$

The results for Survey I are shown in Fig. 14. A similar calculation could not be done effectively for Survey II because of large station-to-station variability in the meridional gradients of $A_{^{210}\mathrm{Po}}$. The fluxes of ^{210}Po measured by drifting sediment traps are also shown. The advective terms for Survey I are important but are less than the Po deficiency term. The relative importance of the

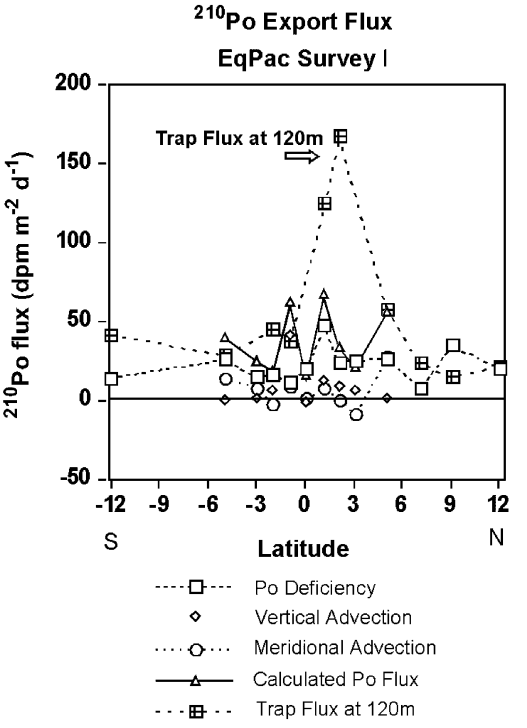

Fig. 14. Export flux of ^{210}Po for Survey I from 12°N to 12°S at 140°W. The Po deficiency flux (□) is compared with contribution due to vertical advection (◇), meridional advection (○) and the measured PIT trap flux (⊞). The total calculated flux with deficiency and transport terms is shown as (△).

advection terms for ^{210}Po is about the same as calculated previously for ^{234}Th (Murray et al., 1996). In general there is good agreement between the trap flux of ^{210}Po and the calculated total flux (including advection terms) except at 2°N and 3°N, where the trap flux is considerably larger. These higher fluxes may be due to the divergence-driven upwelling of deeper water higher in ^{210}Po that can supply additional ^{210}Po for plankton uptake. As for ^{234}Th, the ^{210}Po trap flux is consistently larger than the calculated flux suggesting slight overtrapping of the PIT traps for ^{210}Po. For the El Nino conditions of Survey I, there is little meridional variability in the ^{210}Po export flux.

The ^{210}Po flux can be converted to a carbon flux if we know the C/^{210}Po ratio in sinking particles.

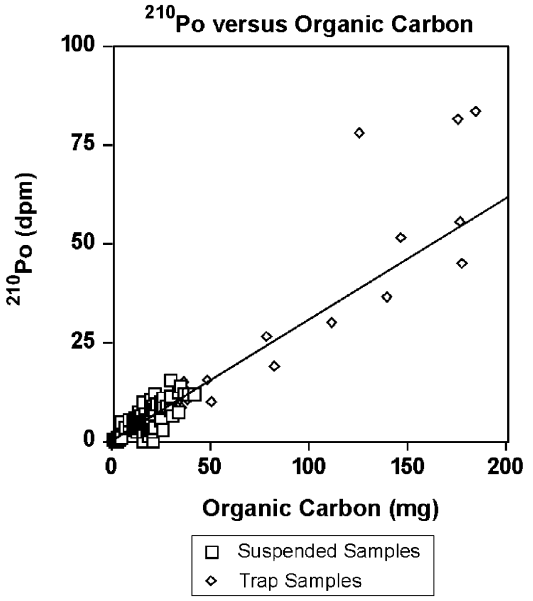

Fig. 15. The correlation of ^{210}Po and organic carbon in suspended particles (□) and PIT trap particles (◇) for EqPac Survey I. The regression shown is: Po (dpm) = 0.307 C (mg) ± 0.550; ($r^2 = 0.637$).

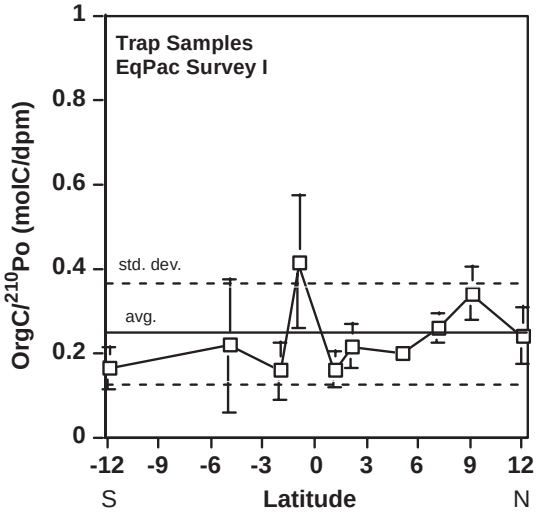

Fig. 16. The organic C to ^{210}Po ratios for individual stations from 12°N to 12°S at 140°W during Survey I. The error bars represent the 1σ standard deviation of values at each station. The solid horizontal line and dotted lines are the mean and standard deviations of all samples.

Biscaye et al. (1988) previously reported a strong correlation between ^{210}Po and organic carbon in deep moored sediment trap samples from the New England margin. The values of ^{210}Po versus organic carbon in both suspended and sediment trap particles are shown in Fig. 15. The correlation is good ($r^2 = 0.637$) and is the same for both types of particles. This is a much stronger correlation than was observed between ^{234}Th and carbon (Murray et al., 1996). In addition, the C/^{234}Th ratios in suspended particles were significantly larger than in trap samples. These differences between ^{210}Po and ^{234}Th are consistent with the hypothesis that ^{210}Po is a better tracer for carbon on the inside of cells, whereas ^{234}Th is related to surface area. It is plausible that recycling plays a more important role for ^{210}Po (and C) than for ^{234}Th. The consistency of the C/^{210}Po ratio suggests that these elements are recycled in a similar manner with little fractionation.

We averaged the C/Po ratios in trap samples at individual stations (shown in Fig. 16 with 1σ error bars). The average value for all samples was 0.25 μmol d^{-1} pm^{-1}. There were no systematic differences with depth. Because individual stations do vary significantly from the mean we used the average for each station rather than the grand average. The same approach was used for the C/Th ratios in Murray et al. (1996).

The organic carbon fluxes for Survey I determined using ^{210}Po were calculated as follows:

$$\text{Model POC flux} = \text{model } ^{210}\text{Po flux} \times (\text{trap POC}/\text{trap } ^{210}\text{Po}). \quad (18)$$

The carbon fluxes as a function of depth are shown in Fig. 17. The stations have been combined in meridional zones of 12–7°N, 5–2°N, 1–1°S, 2–5°S and 7–12°S to simplify the number of symbols in the plot. The results are similar to those presented previously for the export flux calculated using ^{234}Th. Carbon fluxes are either constant or increase with depth from 50 to 250 m. The total range of POC fluxes was from 1–20 mmol C m^{-2} d^{-1}.

Station by station comparison of export carbon fluxes for Survey I by the ^{234}Th and ^{210}Po methods with ^{15}N-new production (McCarthy et al., 1996)

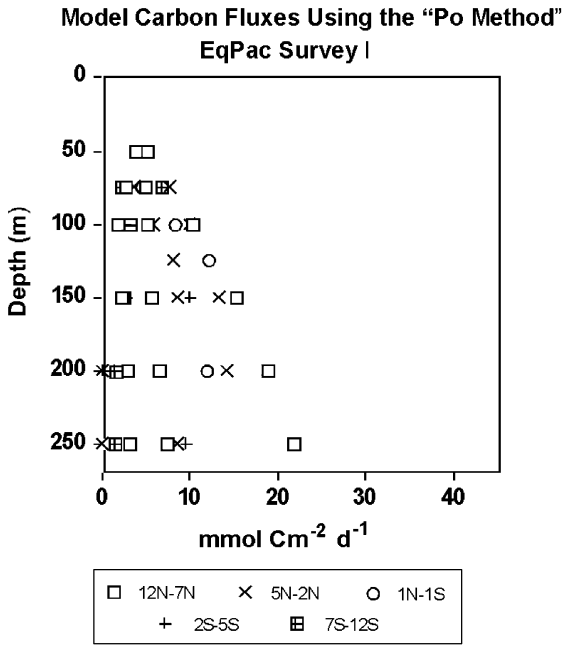

Fig. 17. Organic carbon fluxes from 0 to 250 m for Survey I determined using the "Po-Method".

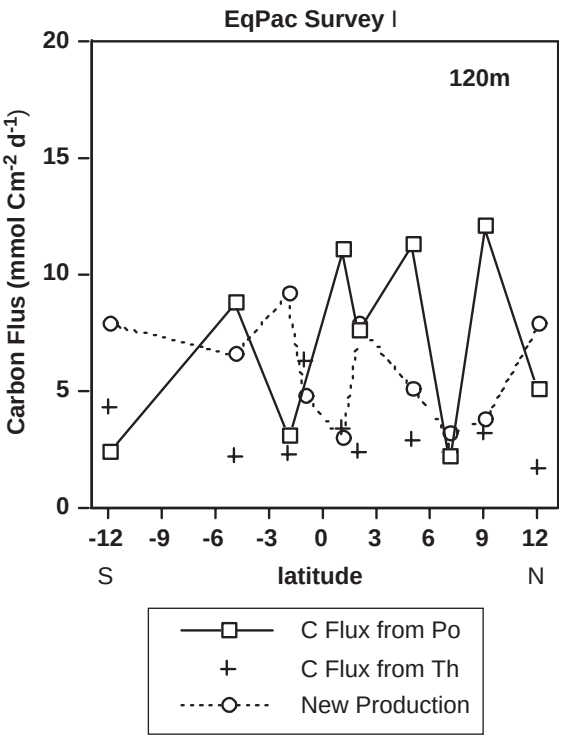

Fig. 18. Comparison of new production (expressed as carbon) (McCarthy et al., 1996) and particulate organic carbon export fluxes (mmol $C\,m^{-2}\,d^{-1}$) determined from ^{234}Th (Murray et al., 1996) and ^{210}Po. All fluxes determined at 120 m during Survey I. The average fluxes from 12°N to 12°S were ^{15}N-new production $= 5.7 \pm 2.1$; ^{234}Th-POC $= 3.4 \pm 1.5$; ^{210}Po-POC $= 7.1 \pm 4.0$ (omitting station).

is shown in Fig. 18. In all cases there is variability in the data but no systematic meridional pattern for this El Nino period. The average fluxes (mmol $C\,m^{-2}\,d^{-1}$) (with std. dev.) at 120 m for Survey I were:

^{15}N-New production $= 5.7 \pm 2.1$,

^{234}Th-POC export $= 3.4 \pm 1.5$,

^{210}Po-POC export $= 7.1 \pm 4.0$,

(excluding station 9 at 1°S).

The uncertainty is larger for the ^{210}Po approach because the advection corrections derived from the station-to-station variability are larger. This uncertainty would be smaller in less dynamic regimes. Because the different approaches integrate over different time scales, perfect agreement would not be expected. The values based on ^{210}Po are higher than the others, probably because the Po-method integrates over the previous 200 d, and POC export for the more normal cold-tongue period prior to the El Nino period of Survey I was probably larger.

Acknowledgements

We appreciate the help of Jan Newton (Washington State Department of Ecology), who was in charge of drifting sediment trap deployments during the EqPac cruises. Kenneth Coale offered us the opportunity to intercalibrate our lead analyses using their trace metal samples. We are grateful for the help of the Captain and crew of R./V. Thompson for their help in collecting samples. This research was supported by NSF OCE 9022466.

Appendix A

Water column data for total ^{226}Ra (calculated from Si) and total, dissolved and particulate ^{234}Th, ^{210}Pb and ^{210}Po: Negative latitudes are south of the equator.

Stn	Lat.	Long.	Depth (m)	^{226}Ra (dpm m^{-3})	Total ^{234}Th ($^{(}$dpm m$^{-3)}$	Diss ^{234}Th (dpm m^{-3})	Part ^{234}Th (dpm m^{-3})	Total ^{210}Pb (dpm m^{-3})	Diss ^{210}Pb (dpm m^{-3})	Part ^{210}Pb (dpm m^{-3})	Total ^{210}Po (dpm m^{-3})	Diss ^{210}Po (dpm m^{-3})	Part ^{210}Po (dpm m^{-3})
Survey I-TT007													
1	11.98	140.08	0	82	2435		366	146		0.8	90		8.2
1	11.98	140.08	50	82	1922	1258	366	142	151	1.6	79	68	15.7
1	11.98	140.08	75	85	2174	1392	365	174	172	0.0	161	123	6.7
1	11.98	140.08	100	92	2471	1606	384	180	163	0.8	180	170	6.3
1	11.98	140.08	150	103	2569	2117	235	155	139	1.6	142	61	6.3
1	11.98	140.08	175	111	2215	2008	213	138	119	1.0	120	58	5.6
1	11.98	140.08	200		2411		217	115		1.1	97		5.4
1	11.98	140.08	250	110	2377	2284	235	124	124	0.8	114	70	6.3
2	9.01	140.09	0	86	1963	1270	353	144	132	0.6	84	46	9.3
2	9.01	140.09	50	86	2046	1219	502	130	118	0.8	74	87	8.1
2	9.01	140.09	75	93	1709	1241	611	154	186	1.4	90	80	7.9
2	9.01	140.09	100	103	2372	1375	637	151	149	0.3	94	116	6.4
2	9.01	140.09	150	109	2545	2145	250	122	124	0.6	65	40	5.3
2	9.01	140.09	175	112	2613	2378	181	123	110	0.3	90	57	2.8
2	9.01	140.09	200	111	2682	2258	179	117		0.0	75		3.4
2	9.01	140.09	250	111	2708	2259	196	105	111	0.0	79	51	3.1
3	7.06	140.02	0	85	2158			109			65		
3	7.06	140.02	25	86	1884			120			76		
3	7.06	140.02	50	85	2268			117			94		
3	7.06	140.02	75	87	2407			153			153		
3	7.06	140.02	100	89	2493			132			149		
3	7.06	140.02	150	105	2369			111			101		
3	7.06	140.02	200	110	2401			117			105		
3	7.06	140.02	250	112	2510			96			99		
4	5.05	140.02	0	86	1767			133			74		
4	5.05	140.02	50	86	1718			122			67		
4	5.05	140.02	75	86	1674			99			76		
4	5.05	140.02	100	87	2466			119			79		
4	5.05	140.02	150	94	2394			142			110		
4	5.05	140.02	175	104	2497			126			122		

4	5.05	140.02	200	109	2443			130			98		
4	5.05	140.02	250	111	2903			107			84		
5	3.01	139.99	0	85	1961	1188	369	125	115	1.0	84	54	12.3
5	3.01	139.99	25	85	1820	1315	324	128	116	1.1	76	35	12.4
5	3.01	139.99	50	85	1944	1760	363	127	172	0.8	68	54	10.9
5	3.01	139.99	75	85	2122	1457	272	119	129	1.0	73	54	8.3
5	3.01	139.99	100	86	2071			106			71		
5	3.01	139.99	125	96	2533			127			126		
5	3.01	139.99	150	100	2594			101			98		
5	3.01	139.99	175	102	2655			105			112		
5	3.01	139.99	225	104	2893			107			96		
5	3.01	139.99	250	106	2639			96			106		
5	3.01	139.99	300	106	0			102			103		
6	2.08	139.92	0	85	1912	1506	280	125	118	1.0	78	45	12.5
6	2.08	139.92	50	85	2244	1619	363	122	112	3.6	80	56	8.7
6	2.08	139.92	75	85	2053	1587	229	105	117	1.0	72	46	8.8
6	2.08	139.92	100	85	2015	2063	198	144	104	20.5	88	42	0.0
6	2.08	139.92	125	86	2630	2423	228	107	105	0.9	101	162	12.5
6	2.08	139.92	150	98	2675	2306	231	121	112	0.9	103	88	8.7
6	2.08	139.92	200	102	2646	2345	206	94	101	0.7	76	97	8.8
6	2.08	139.92	250	105	2489	2318	202	107	105	14.1	79	96	0.0
7	1.13	140.05	0	85	2021	1509	354	136	103	0.7	91	56	12.0
7	1.13	140.05	50	85	2021	1671	360	249	101	0.2	80	51	10.0
7	1.13	140.05	75	85	2038	1626	312	116	113	0.6	73	49	8.8
7	1.13	140.05	100	85	2156	2006	249	126	104	0.6	83	44	5.8
7	1.13	140.05	125	89	2728	2099	174	123	124	1.4	122	88	3.5
7	1.13	140.05	150	100	2388	1872	205	103	104	1.1	101	82	4.1
7	1.13	140.05	200	101	2357	2190	205	106	90	0.9	86	60	5.2
7	1.13	140.05	250	102	2639	2269	206	101	91	1.3	140	61	5.2
8	0.00	140.06	0	84	1775	1700	277	111	102	1.0	78	58	14.0
8	0.00	140.06	50	84	2023	1744	269	107	113	0.8	76	56	12.2
8	0.00	140.06	75	85	2338	1880	243	120	100	0.8	68	55	7.3
8	0.00	140.06	100	85	2522	1732	257	113	106	0.6	76	58	4.6
8	0.00	140.06	125	89	2346	2333	233	97	67	2.9	98	59	4.9
8	0.00	140.06	150	92	2460	2410	177	80	74	1.4	67	77	5.2
8	0.00	140.06	200	97	2795	2457	164	81	80	1.9	70	81	4.2
8	0.00	140.06	250	102	2952	2133	176	95	0	2.5	80	74	10.4
9	−1.02	140.16	0	85	1673						78		
9	−1.02	140.16	50	84	1805						70		
9	−1.02	140.16	75	84	2185	1767	419		82	0.7	92	48	7.0
9	−1.02	140.16	100	85	2231	2211	227			0.7	99	63	5.6

9	−1.02	140.16	125	86	2299						112		
9	−1.02	140.16	150	94	2349	2176	155		78	1.2	100	52	3.1
9	−1.02	140.16	200	101	2422	1971	210		86	1.3	104	44	4.2
9	−1.02	140.16	250	104	2663	2116	184	85		1.0	100	68	3.6
10	−2.02	140.13	0	84	1972	1503	352	99	88	1.0	64	47	11.0
10	−2.02	140.13	50	84	1992	1288	389	101	93	0.5	72	53	8.7
10	−2.02	140.13	75	84	1944	1792	424	99	93	1.1	66	48	9.6
10	−2.02	140.13	100	85	2401	1771	286	104	84		71	45	5.7
10	−2.02	140.13	125	0	2570	2348	252		76	1.2	97	78	5.6
10	−2.02	140.13	150	96	2491	2265	228	82	75	0.6	97	77	2.7
10	−2.02	140.13	200	100	2551	2373	239	82	78	0.6	87	80	4.3
10	−2.02	140.13	250	99	2460	3169	243	75	80	0.3	95	96	4.7
11	−3.00	140.02	0	84	1909			91			66		
11	−3.00	140.02	50	84	1798			88			70		
11	−3.00	140.02	75	84	1970			94			64		
11	−3.00	140.02	100	84	2415			94			65		
11	−3.00	140.02	150	86	2779			76			40		
11	−3.00	140.02	200	99	2625			69			56		
11	−3.00	140.02	250	100	2635			81			60		
12	−5.05	140.00	0	84	2129	1176	621	99	85	0.9	40	40	11.9
12	−5.05	140.00	50	84	1887	1097	1029	99	54	1.3	61	45	9.1
12	−5.05	140.00	75	84	2197	1401	298	93	94	1.1	57	46	9.1
12	−5.05	140.00	100	84	2447	1581	554	101	93	0.5	47	55	6.5
12	−5.05	140.00	125	106	2697	1813	338	74	86	0.2	44	87	3.4
12	−5.05	140.00	150	84	2738	2322	316	71	79	1.2	42	91	2.6
12	−5.05	140.00	200	89	2483	1995	161	76	69	0.6	0	84	1.8
12	−5.05	140.00	250	98	2544	1888	172	75	73	0.6	57	81	4.4
15	−12.03	135.00	0	83	2197	1233	761	105	97	1.1	60	74	3.7
15	−12.03	135.00	25	83	2060	950	766	99	89	0.9	68	63	4.4
15	−12.03	135.00	50	83	2080	1275	719	98	91	0.7	64	49	7.6
15	−12.03	135.00	75	83	2374	1820	371	99	92	1.0	69	68	5.8
15	−12.03	135.00	100	83	2451	2046	350	96	89	0.9	87	91	6.3
15	−12.03	135.00	150	83	2751	2516	210	89	93	0.6	111	102	3.7
15	−12.03	135.00	200	83	2643	2789	253	88	82	2.0	112	69	3.2
15	−12.03	135.00	250	84	2633	2267	150	85	66	0.7	102	79	−0.7
Survey ll−TT011													
1	12.01	140.03	0	82	2138	1805	145	140	125	1.2	80	55	8.7
1	12.01	140.03	25	82	2076	1634	165	141	99	1.2	80	60	9.7
1	12.01	140.03	50	83	2070	1214	250	101	113	1.3	93	59	6.8
1	12.01	140.03	75	83	1889	1599	288	128	135	1.2	112	57	7.7

1	12.01	140.03	100	87	2105	1101	622	159	122	1.0	156	76	3.7
1	12.01	140.03	150	105	2456	1962	199	104	119	0.8	123	121	4.4
1	12.01	140.03	200	107	2479	1590	243	95	91	0.7	106	54	4.7
1	12.01	140.03	250	108	1922	1460	225	68	100	1.2	117	53	5.5
2	8.97	139.97	0	83	1786	1483	343	112	112	1.5	69	54	7.5
2	8.97	139.97	25	83	2160	1058	313	95	102	1.6	55	50	10.1
2	8.97	139.97	50	83	2015	1740	501	123	100	1.7	88	74	8.5
2	8.97	139.97	75	83	1561	1326	361	97	110	2.4	86	63	9.3
2	8.97	139.97	100	89	1848	1209	326	123	129	0.2	64	55	4.1
2	8.97	139.97	150	107	2399	2152	166	96	95	0.5	67	56	0.4
2	8.97	139.97	200	108	2291	2098	216	84	102	1.4	69	66	4.5
2	8.97	139.97	250	108	1949	1597	224	116	121	1.3	74	34	7.2
3	7.01	139.91	0	84	1944			135			71		
3	7.01	139.91	25	84	1815			184			78		
3	7.01	139.91	50	84	0			143			76		
3	7.01	139.91	75	84	1772			152			84		
3	7.01	139.91	100	85	1962			134			111		
3	7.01	139.91	150	101	2387			111			139		
3	7.01	139.91	200	108	2368			85			102		
3	7.01	139.91	250	110	2382			93			91		
4	5.01	139.83	0	85	1651	1047	417	122	118	2.1	67	44	0.0
4	5.01	139.83	25	85	1599	969	500	120	107	1.7	80	48	12.0
4	5.01	139.83	50	85	1566	1097	448	103	92	2.4	72	54	11.6
4	5.01	139.83	75	85	1626	1069	344	120	109	0.9	90	48	7.8
4	5.01	139.83	100	86	1763	1215	253	110	94	0.8	101	85	4.4
4	5.01	139.83	150	95	2453	1739	182	123	111	2.1	155	151	4.0
4	5.01	139.83	200	110	2327	1780	194	110	88	1.7	117	109	6.8
4	5.01	139.83	250	109	2509	1820	133	88	84	2.0	85	87	2.9
5	2.90	140.21	0	83	1591			125			65		
5	2.90	140.21	25	83	1367			126			76		
5	2.90	140.21	50	83	1709			124			83		
5	2.90	140.21	75	84	1928			113			101		
5	2.90	140.21	100	85	1515			95			105		
5	2.90	140.21	150	99	2298			99			99		
5	2.90	140.21	200	101	2235			70			104		
5	2.90	140.21	250	103	2217			90			93		
6-A	2.12	140.24	0	84	1572	1026	294	92	65	2.0	90	60	7.5
6-A	2.12	140.24	25	84	1632			95			87		
6-A	2.12	140.24	50	84	1769	953	293	85	88	1.0	88	83	9.5
6-A	2.12	140.24	75	85	1959			108			87		
6-A	2.12	140.24	100	85	1806	1361	375	92	98	2.5	75	91	3.5

6-A	2.12	140.24	150	85	2386	2061	241	80	99	1.3	67	122	3.3
6-A	2.12	140.24	200	100	2362			80			76		
6-A	2.12	140.24	250	102	2307			76			102		
6-B	2.27	140.87	0	84	3347	931	821	108	89	6.4	96	44	0.0
6-B	2.27	140.87	25	84	1462	996	420	98	78	1.6	94	59	15.6
6-B	2.27	140.87	50	84	1611			78			81		
6-B	2.27	140.87	75	85	1747			96			77		
6-B	2.27	140.87	100	85	2292			88			92		
6-B	2.27	140.87	150	85	2312			73			77		
6-B	2.27	140.87	200	100	2634			82			76		
6-B	2.27	140.87	250	102	2414			84			80		
7	1.14	140.01	0	84	1639			98			91		
7	1.14	140.01	25	84	1634			94			105		
7	1.14	140.01	50	85	1911			97			93		
7	1.14	140.01	75	85	1786			86			110		
7	1.14	140.01	100	86	2209			105			123		
7	1.14	140.01	150	99	2296			73			104		
7	1.14	140.01	200	102	2095			61			104		
7	1.14	140.01	250	102	2396			79			92		
8	0.21	139.90	0	84	1679	904	195	84	76	0.6	85	50	6.8
8	0.21	139.90	25	84	1899	925	273	99	84	1.8	99	75	11.5
8	0.21	139.90	50	84	1948	1020	322	98	60	1.8	112	59	11.2
8	0.21	139.90	75	85	1887	1518	328	96	64	1.7	104	47	2.2
8	0.21	139.90	100	87	2625	1902	277	100	78	2.5	136	110	5.4
8	0.21	139.90	150	96	2524	1778	174	71	76	3.4	111	53	4.4
8	0.21	139.90	200	97	2353	1933	216	91	75	2.8	60	82	4.5
8	0.21	139.90	250	102	2276	1987	221	85	76	2.4	98	94	5.4
8	−1.08	139.96	0	85		957	185		94	1.6		59	9.4
8	−1.08	139.96	25	85		922	355		84	1.6		50	10.5
8	−1.08	139.96	50	85		1029	375		82	1.8		55	11.1
9	−1.08	139.96	75	85		1312	422		69	1.1		50	6.4
9	−1.08	139.96	100	86		2120	265		88	1.2		115	4.2
9	−1.08	139.96	150	91		1490	193		64	2.8		74	5.0
9	−1.08	139.96	200	99		1995	251		71	2.8		75	8.2
9	−1.08	139.96	250	104		1813	254		0	1.8		68	6.0
10	−2.19	140.16	0	85	1426	974	338	97	83	1.5	86	47	13.4
10	−2.19	140.16	25	85	1450	1274	303	84	103	0.5	70	53	5.3
10	−2.19	140.16	50	85	1571	984	319		94	1.2	85	54	10.6
10	−2.19	140.16	75	85	1946	1016	329	92	94	1.1	83	50	7.9
10	−2.19	140.16	100	86	2657	1347	282	80	88	0.7	95	75	5.3
10	−2.19	140.16	150	102	2555	1518	185	92	76	1.1	100	101	3.0

10	−2.19	140.16	200	104	2031	2035	185	75	85	1.2	98	103	4.6
10	−2.19	140.16	250	105	2273	1881	209	77	83	1.0	95	92	4.8
10	−3.22	140.26	0	83	1544			104			85		
10	−3.22	140.26	25	83	1585			100			91		
11	−3.22	140.26	50	84	1383			101			71		
11	−3.22	140.26	75	84	1480			96			96		
11	−3.22	140.26	100	84	1574			81			81		
11	−3.22	140.26	150	100	2327			82			82		
11	−3.22	140.26	200	103	2171			91			83		
11	−3.22	140.26	250	104	2716			83			77		
12	−5.11	140.00	0	83	1485	1000	453	100	75	1.6	77	40	13.4
12	−5.11	140.00	25	83	1536	916	416	94	94	0.9	67	30	5.5
12	−5.11	140.00	50	84	1618	988	313	105	85	0.8	66	47	7.9
12	−5.11	140.00	75	84	1576	1077	383		88	1.9		45	9.1
12	−5.11	140.00	100	83	1534	1265	235	103	81	1.7	81	82	3.4
12	−5.11	140.00	150	83	2125	1454	247	86	93	1.2	69	70	
12	−5.11	140.00	200	89	2494	2056	226	85	76	1.3	85	100	2.1
12	−5.11	140.00	250	99	2253	2226	173	68	66	1.7	68	75	2.9
13	−7.01	138.49	0-A	82	1805			111			4		
13	−7.01	138.49	0-B	0	1925			99			72		
13	−7.01	138.49	50-A	83	1662			31			73		
13	−7.01	138.49	50-B	0	1672			95			62		
13	−7.01	138.49	100-A	83	1907			96			51		
13	−7.01	138.49	100-B	0	1888			88			63		
13	−7.01	138.49	150-A	83	2490			82			66		
13	−7.01	138.49	150-B	0	2357			69			61		
15	−11.93	138.49	0	83	1844	1059	720	99	100	2.6	57	40	11.2
15	−11.93	134.95	25	83	2009	1086	839	102	93	2.1	71	41	12.8
15	−11.93	134.95	50	83	1947	1103	710	102	86	2.9	53	30	11.1
15	−11.93	134.95	75	83	2220	1406	620	102	98	1.3	17	41	6.8
15	−11.93	134.95	100	82	2236	1632	360	89	91	1.9	87	83	4.4
15	−11.93	134.95	150	83	2701	2145	217	92	88	2.7	87	89	2.7
15	−11.93	134.95	200	83	2481	2096	233	95	95	2.8	101	96	2.2
15	−11.93	134.95	250	84	2649	2054	191	96	93	3.8	104	83	4.6

Appendix B

Sediment trap flux data for ^{234}Th, ^{210}Pb, ^{210}Po and organic carbon: Negative latitudes are south of the equator.

Station	Lat (deg)	Long (deg)	Depth (m)	^{234}Th (dpm m^{-2}d^{-1})	^{210}Pb (dpm m^{-2} d^{-1})	^{210}Po (dpm m^{-2} d^{-1})	Org carbon (mmol m^{-2} d^{-1})
Survey I -TT007							
1	11.98	140.08	50	3301	4.9	78.1	10.4
1	11.98	140.08	75	2281	3.0	37.0	11.6
1	11.98	140.08	100	1961	3.4	26.6	6.5
1	11.98	140.08	125	2029			4.8
1	11.98	140.08	150	1083	2.9	15.3	3.0
1	11.98	140.08	175		2.0	16.1	
1	11.98	140.08	200	1040	1.3	10.6	3.2
1	11.98	140.08	250	415	1.5	10.7	2.8
2	9.01	140.09	50	1292	3.2	51.7	12.2
2	9.01	140.09	75	3222	5.8	45.1	14.8
2	9.01	140.09	100	3190	3.0	19.2	6.9
2	9.01	140.09	125	2771			4.3
2	9.01	140.09	150	1600			4.2
2	9.01	140.09	200	1243			2.9
2	9.01	140.09	250	764			2.3
3	7.06	140.02	75	5621	6.0	55.6	14.7
3	7.06	140.02	100	2580	2.5	30.2	9.3
3	7.06	140.02	125	2050		15.2	5.3
3	7.06	140.02	200	1546	3.8	15.6	4.0
3	7.06	140.02	250	1369		13.8	3.0
4	5.05	140.02	75	8361	10.2	83.9	15.3
4	5.05	140.02	100	6585	8.0	81.5	14.6
4	5.05	140.02	125	4501	5.8	21.9	6.5
4	5.05	140.02	200	2540	3.6	15.3	3.5
4	5.05	140.02	250	2333	2.2	13.0	2.8
6	2.08	139.92	75	10510	17.4	90.8	21.5
6	2.08	139.92	100	29333	55.5	237.0	36.0
6	2.08	139.92	125	7478	17.8	63.9	11.4
6	2.08	139.92	200	2312	4.5	15.6	4.4
6	2.08	139.92	250	1653	4.4	17.7	3.7
7	1.13	140.05	75	3157	11.5	73.5	9.0
7	1.13	140.05	100	8313	12.0	105.2	14.9
7	1.13	140.05	125	10783	48.2	155.2	21.0
7	1.13	140.05	200	2183	8.2	25.5	5.6
7	1.13	140.05	250	2701	5.1	22.9	3.9
9	−1.02	140.16	75	2593	1.3	30.6	10.2
9	−1.02	140.16	100	9900	5.9	53.6	12.0
9	−1.02	140.16	150	1495	1.9	13.6	6.3
9	−1.02	140.16	200	1456	0.9	7.3	4.7

9	−1.02	140.16	250	1191	3.1	7.2	3.1
10	−2.02	140.13	75	3062	41.0	87.5	8.2
10	−2.02	140.13	100	3513	3.0	55.5	12.8
10	−2.02	140.13	150	1853	2.6	31.3	2.8
10	−2.02	140.13	200	917	0.6	11.4	1.9
10	−2.02	140.13	250	909	0.6	11.4	2.5
12	−5.05	140.00	75	1682	1.4	56.0	6.3
12	−5.05	140.00	100	1721	0.6	32.4	3.4
12	−5.05	140.00	150	1297	0.4	24.3	3.5
12	−5.05	140.00	200	952	1.3	12.4	3.3
12	−5.05	140.00	250	1000	2.9	6.3	3.0
15	−12.03	135.00	75	1052	3.1	38.1	6.0
15	−12.03	135.00	100	1493	1.7	53.2	5.4
15	−12.03	135.00	150	1068	0.0	25.5	3.9
15	−12.03	135.00	200	588	1.5	18.6	3.3
15	−12.03	135.00	250	635	2.8	13.6	3.2
Survey II -TT011							
1	12.01	140.03	75	1283	3.08	36.51	14.65
1	12.01	140.03	100	1414	3.59	25.44	7.15
1	12.01	140.03	150	1759	2.74	19.37	5.06
1	12.01	140.03	200	955	3.09	13.52	3.85
1	12.01	140.03	250	853	1.53	10.47	2.60
2	8.97	139.97	75	1357	3.81	27.51	5.61
2	8.97	139.97	100	2342	5.49	34.89	8.80
2	8.97	139.97	150	3914			3.40
2	8.97	139.97	200	1676	2.76	17.02	2.33
2	8.97	139.97	250	939	1.11	14.16	2.83
3	7.01	139.91	75	1319	3.24	50.64	7.99
3	7.01	139.91	100	1854	5.22	28.05	5.47
3	7.01	139.91	150	1492	5.18	19.75	3.22
3	7.01	139.91	200	1016			3.08
3	7.01	139.91	250	912	4.73	16.12	3.56
4	5.01	139.83	75	3260	5.31	71.14	7.62
4	5.01	139.83	100	4057	6.17	57.21	15.10
4	5.01	139.83	150	1733	5.34	61.86	8.42
4	5.01	139.83	200	1913	5.05	25.11	7.85
4	5.01	139.83	250	1901	4.25	43.59	6.38
5	2.90	140.21	75	3484	9.73	72.71	21.27
5	2.90	140.21	100	5786	11.13	78.94	14.46
5	2.90	140.21	150	2637	6.05	29.13	7.50
5	2.90	140.21	200	1427	4.89	23.84	5.65
5	2.90	140.21	250	1388	3.85	25.61	5.18
6-A	2.12	140.24	75	3440	10.94	433.56	41.11
6-A	2.12	140.24	100	4261	11.27	152.32	33.43
6-A	2.12	140.24	150	1976	8.85	52.12	11.05
6-A	2.12	140.24	200	1901	6.94		10.56
6-A	2.12	140.24	250	1762	7.36	36.98	6.20

6-B	2.27	140.87	75	3440	10.94	433.56	41.11
6-B	2.27	140.87	100	4261	11.27	152.32	33.43
6-B	2.27	140.87	150	1976	8.85	52.12	11.05
6-B	2.27	140.87	200	1901	6.94		10.56
6-B	2.27	140.87	250	1762	7.36	36.98	6.20
Survey II -	TT011						
7	1.14	140.01	100	5716	13.50	447.48	28.72
7	1.14	140.01	125	2940	12.10	53.26	14.96
7	1.14	140.01	150	2729	11.78	39.67	13.53
7	1.14	140.01	200	2501	9.31	35.01	12.60
7	1.14	140.01	250	2653	10.22	31.47	13.60
8	0.21	139.9	100	3097	7.49	108.43	6.39
8	0.21	139.9	125	1770	6.08	23.56	5.16
8	0.21	139.9	150	2198	6.79	28.61	6.82
8	0.21	139.9	200	2094	7.00	21.94	5.51
8	0.21	139.9	250	1057	8.18	30.55	4.60
9	−1.07	139.95	100	3257	7.71	33.03	8.29
9	−1.07	139.95	125	3206	14.11	81.41	5.73
9	−1.07	139.95	150	2108	8.28		3.99
9	−1.07	139.95	200	1902	7.54	24.93	4.44
9	−1.07	139.95	250	1300	6.59	21.61	4.90
10	−2.19	140.16	100	5213	9.55	46.24	14.63
10	−2.19	140.16	125	3454	3.58	43.78	11.58
10	−2.19	140.16	150	2918	8.02	27.84	6.44
10	−2.19	140.16	200	3878	7.28	22.70	5.71
10	−2.19	140.16	250	2844	7.34	18.69	4.69
11	−3.22	140.26	100	3773		67.65	20.49
11	−3.22	140.26	125	3231	8.79	38.70	15.18
11	−3.22	140.26	150	2825	9.95	35.04	8.08
11	−3.22	140.26	200	3175	8.77	29.16	5.86
11	−3.22	140.26	250	5042	11.09	28.86	9.21
12	−5.11	140	100	5015	18.98	64.77	29.06
12	−5.11	140	125	5749	84.37	74.02	29.44
12	−5.11	140	150	6179	13.13	78.71	22.49
12	−5.11	140	200	2961	5.28	14.49	10.41
12	−5.11	140	250	6357	6.62	38.06	5.95
15	−11.93	134.95	100	1663	4.70	20.99	4.04
15	−11.93	134.95	125	4482	6.18	26.45	12.38
15	−11.93	134.95	150	3663	7.60	23.03	10.74
15	−11.93	134.95	200	3135	5.92	16.30	4.32
15	−11.93	134.95	250	643	4.50	16.71	4.46

References

Anderson, R.F., Fleer, A.P., 1982. Determination of natural activities of thorium and plutonium in marine particle matter. Analytical Chemistry 54, 1142–1147.

Aufdenkampe, A.K., McCarthy, J.J., Rodier, M., Navarette, C., Dunne, J., Murray, J.W., 2001. Estimation of new production in the tropical Pacific. Global Biogeochemical Cycles 15, 101–112.

Bacon, M.P., Spencer, D.W., Brewer, P.G., 1976. Pb-210/Ra-226 and Po-210/Pb-210 disequilibria in seawater and suspended particulate matter. Earth and Planetary Science Letters 32, 277–296.

Bacon, M.P., Belastock, R.A., Tecotzky, M., Turekian, K.K., Spencer, D.W., 1988. Lead-210 and polonium-210 in ocean water profiles of the continental shelf and slope south of New England. Continental Shelf Research 8, 841–853.

Bacon, M.P., Cochran, J.K., Hirschberg, D., Hammer, T.R., Fleer, A.P., 1996. Export flux of carbon at the equator during the EqPac time series cruises estimated from ^{234}Th measurements. Deep-Sea Research II 43, 1133–1154.

Balkanski, Y.J., Jacob, D.J., Gardner, G.M., Graustein, W.C., Turekian, K.K., 1993. Transport and residence times of tropospheric aerosols inferred from a global three-dimensional simulation of ^{210}Pb. Journal of Geophysical Research 98, 20,573–20,586.

Bhat, S.G., Krishnaswami, S., Lal, D., Rama, Moore, W.S., 1969. ^{234}Th/^{238}U ratios in the ocean. Earth and Planetary Science Letters 5, 483–491.

Biscaye, P.E., Anderson, R.F., Deck, B.L., 1988. Fluxes of particles and constituents to the eastern United States continental slope and rise: SEEP-1. Continental Shelf Research 8, 855–904.

Bollhöfer, A., Rosman, K.J.R., 2001. Isotope source signatures for atmospheric lead: The Northern Hemisphere. Geochimica et Cosmochimica Acta 65, 1727–1740.

Boyle, E.A., Chapnick, S.D., Shen, G.T., Bacon, M.P., 1986. Temporal variability of lead in the western North Atlantic. Journal of Geophysical Research 91, 8573–8593.

Boyle, E.A., Sherrell, R.M., Bacon, M.P., 1994. Lead variability in the western North Atlantic Ocean and central Greenland ice: implications for the search for decadal trends in anthropogenic emissions. Geochimica et Cosmochimica Acta 58, 3227–3238.

Bruland, K.W., Coale, K.H., 1986. Surface water ^{234}Th/^{238}U disequilibrium: spatial and temporal variations of scavenging rates within the Pacific Ocean. In: Burton, J.D., Brewer, P.G., Cheselet, E. (Eds.), Dynamic processes in the chemistry of the upper ocean. Plenum, New York, pp. 159–172.

Buesseler, K.O., Bacon, M.P., Cochran, J.K., Livingston, H.D., 1992. Carbon and nitrogen export during the JGOFS North Atlantic Bloom Experiment estimated from ^{234}Th:^{238}U disequilibria. Deep-Sea Research I 42, 619–639.

Buesseler, K.O., Andrews, J.A., Hartman, M.C., Belastock, R., Chai, F., 1995. Regional estimates of the export flux of organic carbon derived from thorium-234 during the JGOFS EqPac program. Deep-Sea Research II 42, 777–804.

Chai, F., 1995. Origin and maintenance of a high nitrate condition in the equatorial Pacific. A biological-physical model study. Ph.D. Thesis, Duke University, 170pp.

Chapin, T.P., 1997. On-line preconcentration and interference removal for the analysis of trace metals in seawater by flow injection inductively coupled plasma mass spectrometry. Analytical Chemistry.

Chapin, T.P., 1997. Trace metal cycling in the central equatorial Pacific: results from the U.S. JGOFS EqPac Survey Cruises. Ph.D. Thesis, University of Washington, 243pp.

Charette, M.A., Moran, S.B., 1999. Rates of particle scavenging and particulate organic carbon export estimated using ^{234}Th as a tracer in the subtropical and equatorial Atlantic Ocean. Deep-Sea Research II 46, 885–906.

Chen, J.H., Edwards, R.L., Wasserburg, G.J., 1986. ^{238}U, ^{234}U and ^{232}Th in seawater. Earth and Planetary Science Letters 80, 241–251.

Cherry, R.D., Heyraud, M., 1991. Polonium-210 in selected categories of marine organisms: interpretation of the data on the basis of an unstructured marine food web model. In: Kershaw, P.J., Woodhead, D.S. (Eds.), Radionuclides in the Study of Marine Processes. Elsevier, Amsterdam, pp. 362–372.

Chung, Y., Craig, H., 1980. ^{226}Ra in the Pacific Ocean. Earth and Planetary Science Letters 49, 267–292.

Chung, Y., Craig, H., 1983. ^{210}Pb in the Pacific: the GEOSECS measurements of particulate and dissolved concentrations. Earth and Planetary Science Letters 65, 406–432.

Clegg, S.L., Whitfield, M., 1990. A generalized model for the scavenging of trace metals in the open ocean—I. Particle cycling. Deep-Sea Research 37, 809–832.

Clegg, S.L., Whitfield, M., 1991. A generalized model for the scavenging of trace metals in the open ocean—II. Thorium scavenging. Deep-Sea Research 38, 91–120.

Clegg, S.L., Whitfield, M., 1993. Application of a generalized scavenging model to time series ^{234}Th and particle data obtained during the JGOFS North Atlantic Bloom Experiment. Deep-Sea Research 40, 1529–1545.

Coale, K.H., Bruland, K.W., 1985. ^{234}Th:^{238}U disequilibria within the California Current. Limnology and Oceanography 30, 22–33.

Craig, H., Krishnaswami, S., Somayajulu, B.L.K., 1973. Pb-210/Ra-226: radioactive disequilibria in the deep sea. Earth and Planetary Science Letters 17, 295–305.

Dunne, J.P., Murray, J.W., 1999. Sensitivity of ^{234}Th export to physical processes in the central equatorial Pacific. Deep-Sea Research I 46, 831–854.

Dunne, J.P., Murray, J.W., Young, J., Balistrieri, L.S., Bishop, J., 1997. ^{234}Th and particle cycling in the central equatorial Pacific. Deep-Sea Research II 44, 2049–2084.

Fisher, N.S., Burns, K.A., Cherry, R.D., Heyraud, M., 1983. Accumulation and cellular distribution of ^{241}Am, ^{210}Pb and ^{210}Po in two marine algae. Marine Ecology-Progress Series 11, 233–237.

Fleer, A.P., Bacon, M.P., 1984. Determination of lead-210 and polonium-210 in seawater and marine particulate matter. Nuclear Instruments and Methods in Physics Research 223, 243–249.

Flegal, A.R., Patterson, C.C., 1983. Vertical concentration profiles of lead in the Central Pacific at 15°N and 20°S. Earth and Planetary Science Letters 64, 19–32.

Friederich, J., Rutgers van der Loeff, M.M., 2002. A two-tracer (^{210}Po–^{234}Th) approach to distinguish organic carbon and biogenic silica export flux in the Antarctic Circumpolar Current. Deep-Sea Research I 49, 101–120.

Guo, L., Chen, M., Gueguen, C., 2002. Control of Pa/Th ratio by particulate chemical composition. Geophysical Research Letters 29, 1960.

Harada, K., Tsunogai, S., 1986. Fluxes of ^{234}Th, ^{210}Pb and ^{210}Po determined by sediment trap experiments in Pelagic Oceans. Journal of the Oceanographic Society of Japan 42, 192–200.

Heyraud, M., Cherry, R.D., 1979. Polonium-210 and lead-210 in marine food chains. Marine Biology 52, 227–236.

Heyraud, M., Fowler, S.W., Beasley, T.M., Cherry, R.D., 1976. Polonium-210 in ephausids: a detailed study. Marine Biology 34, 127–138.

Honeyman, B.D., Santschi, P.H., 1989. A Brownian-pumping model for oceanic trace metal scavenging: evidence from Th isotopes. Journal of Marine Research 47, 951–992.

Honeyman, B.D., Balistrieri, L.S., Murray, J.W., 1988. Oceanic trace metal scavenging: the importance of particle concentration. Deep-Sea Research 35, 227–246.

Hussain, N., Church, T.M., Véron, A.J., Larson, R.E., 1998. Radon daughter disequilibria and lead systematics in the western North Atlantic. Journal of Geophysical Research 103 (D13), 16,059–16,071.

Jones, C.E., Halliday, A.N., Rea, D.K., Owen, R.M., 2000. Eolian inputs of lead to the North Pacific. Geochimica et Cosmochimica Acta 64, 1405–1416.

Kadko, D., 1993. Excess ^{210}Po and nutrient recycling within the California coastal transition zone. Journal of Geophysical Research 98, 857–864.

Kharkar, D.P., Thomson, J., Turekian, K.K., Foster, W.O., 1976. Uranium and thorium decay series nuclides in plankton from the Caribbean. Limnology and Oceanography 21, 294–299.

Kim, G., Church, T.M., 2001. Seasonal biogeochemical fluxes of ^{234}Th and ^{210}Po in the upper Sargasso Sea: influence from atmospheric iron deposition. Global Biogeochemical Cycles 15, 651–661.

Kim, G., Alleman, L.Y., Church, T.M., 1999. Atmospheric depositional fluxes of trace elements, ^{210}Pb and ^{7}Be to the Sargasso Sea. Global Biogeochemical Cycles 13, 1183–1192.

Knauer, G.A., Karl, D.M., Martin, J.H., Hunter, C.N., 1990. Fluxes of particulate carbon, nitrogen and phosphorus in the upper water column of the northeast Pacific. Deep-Sea Research 26, 97–108.

Ku, T.-L., Lin, M.-C., 1976. ^{226}Ra distribution in the Antarctic Ocean. Earth and Planetary Science Letters 32, 236–248.

Ku, T.-L., Luo, S., Kusakabe, M., Bishop, J.K.B., 1995. ^{228}Ra-derived nutrient budgets in the upper equatorial Pacific and the role of "new" silicate in limiting productivity. Deep-Sea Research II 42, 479–498.

Landing, W.M., Haraldsson, C., Paxens, N., 1986. Vinyl polymer agglomerate based transition metal cation chelating ion-exchange resin containing the 8-hydroxyquinoline functional group. Analytical Chemistry 58, 3031–3035.

Maring, H., Patterson, C., Settle, D., 1989. Atmospheric input fluxes of industrial and natural Pb from the westerlies to the mid-north Pacific. In: Duce, R.A. (Ed.), Chemical Oceanography: SEAREX: The Sea/Air Exchange Program, Vol. 10. Academic Press, New York, pp. 83–106.

Matsumoto, E., 1975. ^{234}Th-^{238}U radioactive disequilibrium in the surface layer of the ocean. Geochimica et Cosmochimica Acta 39, 205–212.

McCarthy, J.J., Garside, C., Nevins, J.L., Barber, R.T., 1996. New Production along 140°W in the equatorial Pacific during and following the 1992 El Niño event. Deep-Sea Research II 43, 1065–1094.

Murnane, R.J., Sarmiento, J.L., Bacon, M., 1990. Thorium isotopes, particle cycling models and inverse calculations of model rate constants. Journal of Geophysical Research 95, 16,195–16,206.

Murnane, R.J., Cochran, J.K., Sarmiento, J.L., 1994a. Estimates of particle- and thorium-cycling rates in the northwest Atlantic Ocean. Journal of Geophysical Research 99, 3373–3392.

Murnane, R.J., Cochran, J.K., Sarmiento, J.L., 1994b. Determination of thorium and particulate matter cycling parameters at Station P: a reanalysis and comparison of least squares techniques. Journal of Geophysical Research 99, 3393–3405.

Murozumi, M., Chow, T.J., Patterson, C.C., 1969. Chemical concentrations of pollutant lead aerosols, terrestrial dusts and sea salts in Greenland and Antarctic snow strata. Geochimica et Cosmochimica Acta 33, 1247–1294.

Murray, J.W., Downs, J.N., Strom, S., Wei, C.-L., Jannasch, H.W., 1989. Nutrient assimilation, export production and ^{234}Th scavenging in the eastern equatorial Pacific. Deep-Sea Research 36, 1471–1489.

Murray, J.W., Barber, R.T., Roman, M.R., Bacon, M.P., Feely, R.A., 1994. Physical and biological controls on carbon cycling in the equatorial Pacific. Science 266, 58–65.

Murray, J.W., Johnson, E., Garside, C., 1995. A US JGOFS Process Study in the equatorial Pacific (EqPac): introduction. Deep-Sea Research II 42, 275–293.

Murray, J.W., Young, J., Newton, J., Dunne, J., Chapin, T., Paul, B., McCarthy, J.J., 1996. Export flux of particulate organic carbon from the central equatorial Pacific determined using a combined drifting trap-^{234}Th approach. Deep-Sea Research II 41, 1095–1132.

Nozaki, Y., Tsunogai, S., 1976. ^{226}Ra, ^{210}Pb and ^{210}Po disequilibria in the western North Pacific. Earth Planetary Science Letters 32, 313–321.

Nozaki, Y., Thomson, J., Turekian, K.K., 1976. The distribution of Pb-210 and Po-210 in the surface waters of the Pacific Ocean. Earth Planet Science Letters 32, 304–312.

Nozaki, Y., Ikuta, N., Yashima, M., 1990. Unusually large ^{210}Po deficiencies relative to ^{210}Pb in the Kuroshiro Current of the East China and Philippine Seas. Journal of Geophysical Research 95, 5321–5329.

Nozaki, Y., Zhang, J., Takeda, A., 1997. ^{210}Pb and ^{210}Po in the equatorial Pacific and the Bering Sea: the effects of biological productivity and boundary scavenging. Deep-Sea Research II 44, 2203–2220.

Nozaki, Y., Dobashi, F., Kato, Y., Yamamoto, Y., 1998. Distribution of Ra isotopes and the ^{210}Pb and ^{210}Po balance in surface seawaters of the mid-Northern hemisphere. Deep-Sea Research I 45, 1263–1284.

Nriagu, J.O., 1989. The history of leaded gasoline. In: Vernet, J.-P. (Ed.), Heavy Metals in the Environment. Page Bros, pp. 361–366.

Patterson, C.C., Settle, D.M., 1987. Review of data on eolian fluxes of industrial and natural lead to the lands and seas in remote regions on a global scale. Marine Chemistry 22, 137–162.

Philander, S.G.H., Gu, D., Halpern, D., Lau, N.-C., Li, T., Pacanowski, R.C., 1996. Why the ITCZ is mostly north of the equator. Journal of Climate 9, 2958–2972.

Quigley, M.S., Santschi, P.H., Hung, C.-C., Guo, L., Honeyman, B.D., 2002. Importance of polysaccharides for ^{234}Th complexation to marine particulate matter. Limnology and Oceanography 47, 367–377.

Rea, D.K., 1994. The paleoclimate record provided by eolian deposition in the deep sea: the global history of wind. Reviews of Geophysics 32, 159–195.

Sanderson, M.P., Hunter, C.N., Fitzwater, S.E., Gordon, R.M., Barber, R.T., 1995. Primary productivity and trace-metal contamination measurements from a clean rosette system versus ultra-clean Go-Flo bottles. Deep-Sea Research II 42, 431–440.

Sarin, M.M., Kim, G., Church, T.M., 1999. ^{210}Po and ^{210}Pb in the south-equatorial Atlantic: distribution and disequilibrium in the upper 500 m. Deep-Sea Research II 46, 907–917.

Schaule, B.K., Patterson, C.C., 1981. Lead concentrations in the northeast Pacific: evidence for global anthropogenic perturbations. Earth and Planetary Science Letters 54, 97–116.

Schaule, B.K., Patterson, C.C., 1983. Perturbations of the natural Pb depth profile in the Sargasso Sea by industrial lead. In: Wong, C.S., Boyle, E.A., Bruland, K., Burton, D., Goldberg, E.D. (Eds.), Trace Elements in Seawater. Plenum, New York, pp. 487–504.

Settle, D.M., Patterson, C.C., Turekian, K.K., Cochran, J.K., 1982. Magnitudes and sources of precipitation and dry deposition of industrial and natural Pb to the North Pacific at Enewetak. Journal of Geophysical Research 87, 8857–8869.

Shannon, L.V., Cherry, R.D., Cherry, M.J., 1970. Polonium-210 and lead-210 in the marine environment. Geochimica et Cosmochimica Acta 34, 701–711.

Shen, G.T., Boyle, E.A., 1988. Thermocline ventilation of anthropogenic lead in the western North Atlantic. Journal of Geophysical Research 93, 15,715–15,732.

Sherrell, R.M., Boyle, E.A., Hamelin, B., 1992. Isotopic equilibration between dissolved and suspended particulate lead in the Atlantic Ocean: evidence from ^{210}Pb and stable Pb isotopes. Journal of Geophysical Research 97, 11,257–11,268.

Shimmield, G.B., Ritchie, G.D., Fileman, T.W., 1995. The impact of marginal ice zone processes on the distribution of ^{210}Pb, ^{210}Po and ^{234}Th and implications for new production in the Bellinghausen Sea, Antarctica. Deep-Sea Research II 42, 1313–1335.

Shotyk, W., Weiss, D., Appleby, P.G., Cheburkin, A.K., Frei, R., Gloor, M., Kramers, J.D., Reese, S., van der Knaap, W.O., 1998. History of atmospheric lead deposition since 12,370 ^{14}C yr BP from a Peat Bog, Jura Mountains, Switzerland. Science 281, 1635–1640.

Spencer, D.W., Bacon, M.P., Brewer, P.G., 1981. Models of the distribution of Pb-210 in a section across the north equatorial Atlantic Ocean. Journal of Marine Research 39, 119–138.

Stewart, G.M., Fisher, N.S., 2003a. Experimental studies on the accumulation of polpnium-210 by marine phytoplankton. Limnology and Oceanography 48, 1193–1201.

Stewart, G.M., Fisher, N.S., 2003b. Bioaccumulation of polonium-210 in marine copepods. Limnology and Oceanography 48, 2011–2019.

Tanaka, N., Takeda, Y., Tsunogai, S., 1983. Biological effect on removal of Th-234, Po-210 and Pb-210 from surface water in Funka Bay, Japan. Geochimica et Cosmochimica Acta 47, 1783–1790.

Turekian, K.K., Cochran, J.K., 1981. Pb-210 in surface air at Enewetak and the Asian dust flux to the Pacific. Nature 292, 522–524.

Turekian, K.K., Kharkar, D.P., Thomson, J., 1974. The fates of Pb-210 and Po-210 in the surface ocean. Journal de Recherches Atmospheriques 8, 639–646.

Turekian, K.K., Nozaki, Y., Benninger, L.K., 1977. Geochemistry of radon and radon products. Annual Reviews in Earth and Planetary Science 5, 227–255.

Turekian, K.K., Graustein, W.C., Cochran, J.K., 1989. Lead-210 in the SEAREX program: an aerosol tracer across the Pacific. In: Duce, R.A. (Ed.), Chemical Oceanography; SEAREX: The Sea/Air Exchange Program. Academic Press, New York, pp. 51–81.

Veron, A., Church, T., Flegal, R., Patterson, C.C., Erel, Y., 1993. Response of lead cycling in the surface Sargasso Sea to changes in atmospheric input. Journal of Geophysical Research 98 (C10), 18,269–18,276.

Wei, C.-L., Murray, J.W., 1994. The behavior of scavenged isotopes in marine anoxic environments: ^{210}Pb and ^{210}Po in the water column of the Black Sea. Geochemica et Cosmochimica Acta 58, 1795–1811.